

Research paper

Relaxed inertial subgradient extragradient methods for equilibrium problems in Hilbert spaces and their applications to image restoration

Habib ur Rehman ^a, Bing Tan ^b, Jen-Chih Yao ^c

^a School of Mathematical Sciences, Zhejiang Normal University, Jinhua, 321004, China

^b School of Mathematics and Statistics, Southwest University, Chongqing, 400715, China

^c Center for General Education, China Medical University, Taichung, Taiwan and Academy of Romanian Scientists, Romania

ARTICLE INFO

MSC:
65J15
47H05
47J25
47J20

Keywords:
Pseudomonotone bifunction
Subgradient extragradient method
Equilibrium problem
Image restoration problem

ABSTRACT

We introduce two extragradient methods that incorporate one-step inertial terms and self-adaptive step sizes for equilibrium problems in real Hilbert spaces. These methods synergistically combine inertial techniques and relaxation parameters to enhance convergence speed while ensuring superior performance in addressing pseudomonotone and Lipschitz continuous equilibrium problems. The first method is formulated to achieve weak convergence, whereas the second method guarantees strong convergence; both methods feature designed step-size adaptation mechanisms that maintain feasibility and efficiency. The proposed methods utilize adaptive step sizes that are updated at each iteration based on previous iterations. Convergence is demonstrated under mild assumptions, and our findings generalize and extend some related results within the existing literature. Lastly, we present numerical experiments that illustrate the performance of the proposed methods, including their applications to image restoration problems.

1. Introduction

Let \mathcal{H} be a real Hilbert space endowed with an inner product $\langle \cdot, \cdot \rangle$ and an induced norm $\|\cdot\|$, and let $C \subseteq \mathcal{H}$ be a nonempty, closed, and convex subset. The equilibrium problem aims to identify a solution x^* within a subset C of a real Hilbert space \mathcal{H} such that this solution satisfies a specified inequality for all elements in C . Formally, the problem is defined as follows: assume there exists a bifunction $B : \mathcal{H} \times \mathcal{H} \rightarrow \mathbb{R}$ such that $B(s, s) = 0$ for any $s \in C$. The objective is to find an element $x^* \in C$ that satisfies the inequality

$$B(x^*, s) \geq 0, \quad \text{for all } s \in C. \quad (\text{EP})$$

Equilibrium problems offer a framework for handling various classical challenges in optimization and mathematical programming, such as variational inequalities, convex programming, optimization with equilibrium constraints, and specific game-theoretic models [1,2]. The equilibrium problem framework is indispensable across various fields, including economics and game theory. Nash's seminal work [3] exemplifies how equilibrium can model interactions among competing agents, establishing a foundational concept in these disciplines.

* Corresponding author.

E-mail addresses: hrehman@zjnu.edu.cn (H.u. Rehman), bingtan@swu.edu.cn (B. Tan), yaojc@mail.cmu.edu.tw (J.-C. Yao).

The auxiliary problem principle, first introduced by Cohen [4] for optimization problems, was subsequently extended to variational inequality problems [5]. Mastroeni [6] further applied this principle to equilibrium problems characterized by strongly monotone bifunctions. An initial method based on this principle for solving equilibrium problems was proposed by Flåm and Antipin [7]. This convergence analysis operates under the assumption that the bifunction \mathcal{B} is pseudomonotone and adheres to a Lipschitz-type condition. Specifically, there exist positive constants c_1 and c_2 such that, for all $s_1, s_2, s_3 \in C$,

$$\mathcal{B}(s_1, s_3) \leq \mathcal{B}(s_1, s_2) + \mathcal{B}(s_2, s_3) + c_1 \|s_1 - s_2\|^2 + c_2 \|s_2 - s_3\|^2. \quad (\text{L-type})$$

The extragradient method is an iterative optimization technique designed to address both variational inequality problems and equilibrium problems. Specifically, as delineated in [8], the extragradient method generates two sequences, $\{x_k\}$ and $\{y_k\}$, in the following manner. Initiating from an arbitrary point x_0 within the feasible set C , the method updates iteratively as follows:

$$\begin{cases} x_k \in C, \\ y_k = \arg \min_{s \in C} \left\{ \varpi \mathcal{B}(x_k, s) + \frac{1}{2} \|x_k - s\|^2 \right\}, \\ x_{k+1} = \arg \min_{s \in C} \left\{ \varpi \mathcal{B}(y_k, s) + \frac{1}{2} \|x_k - s\|^2 \right\}, \end{cases} \quad (1)$$

where ϖ is a positive parameter. The performance and convergence of the extragradient method are contingent upon the judicious selection of the parameter ϖ , which must satisfy $0 < \varpi < \min \left\{ \frac{1}{2c_1}, \frac{1}{2c_2} \right\}$, where c_1 and c_2 are the Lipschitz constants. Note that

the approach described in (1) requires solving the optimization problem on the feasible set twice per iteration. Moreover, it relies on a fixed step size, which is determined based on prior knowledge or an estimate of the Lipschitz constant of the bifunction. Additionally, the method guarantees only weak convergence in Hilbert spaces.

The extragradient method [9] continues to be one of the most widely utilized techniques for addressing variational inequality problems and equilibrium problems. This two-step iterative procedure was designed to overcome the limitations of classical projection methods, particularly in non-monotone contexts, by executing two projections in each iteration instead of one. This modification significantly enhances both the convergence rate and robustness of the method. Subsequently, a method known as the subgradient extragradient algorithm was introduced by Censor et al. [10–12]. In this approach, the projection onto the feasible set in the second step is replaced by a projection onto a half-space (with a formal expression provided). This modification implies that, in each iteration, the method only requires one computation of the projection onto the feasible set, which significantly improves the computational efficiency of the extragradient algorithm.

Inertial method [13] represent a class of optimization algorithms that enhance convergence rates by incorporating a memory term that utilizes information from prior iterations. Drawing inspiration from Nesterov's accelerated gradient method [14] and the work of Alvarez and Attouch [15]. On the other hand, relaxation method is also widely used by scholars as an acceleration technique. Recently, researchers have combined the relaxation technique, the inertial methods, the extragradient algorithm, and the subgradient extragradient algorithms to solve equilibrium problems; see, e.g., [16–24].

It is noted that the algorithm in [25] are designed to solve monotone equilibrium problems, while the algorithms in [8, 16, 17, 20, 26–30] are intended for pseudomonotone equilibrium problems. As is well known, pseudomonotone bifunctions include monotone bifunctions, thus the algorithms mentioned above have a broader range of applicability. On the other hand, researchers have also proposed algorithms that do not require any monotonicity to solve equilibrium problems; see, e.g., [31–34].

The preceding discussion leads to the following natural question:

Is it possible to modify the method in (1) by incorporating relaxation parameters and inertial terms to achieve both weak and strong convergence when solving equilibrium problems without monotonicity?

In this paper, we give a positive answer to the above question. Specifically, our contributions are as follows:

- (1) We propose two new relaxed inertial-type methods for solving the problem (EP) in real Hilbert spaces. We demonstrate that the proposed methods converge weakly and strongly, respectively, when the bifunction is pseudomonotone and Lipschitz continuous. Additionally, our methods achieve weak and strong convergence independently of the Lipschitz constant of the bifunction. Both methods incorporate adaptive step-size mechanisms, ensuring their applicability to a broad range of problem settings.
- (2) Numerical comparisons of our methods with relevant approaches to equilibrium problems, utilizing test cases derived from image restoration problems, demonstrate that our methods are efficient.

The structure of this paper is as follows: In Section 2, we review key definitions and preliminary results that will be utilized in subsequent sections. Section 3 is dedicated to analyzing the convergence of the proposed algorithms. In Section 4, we present several numerical examples to illustrate the performance of our algorithms. Finally, we give a summary of this paper in Section 5.

2. Preliminaries

This section presents a comprehensive review of the fundamental concepts and results that are employed throughout this paper. We denote weak convergence of the sequence $\{x_k\}$ to x by $x_k \rightharpoonup x$ and strong convergence by $x_k \rightarrow x$. The normal cone to the set C at a point $x \in C$ is represented by $N_C(x)$. Let $\varphi : C \rightarrow \mathbb{R}$ be a convex function. The subdifferential of φ at $x \in C$ is denoted by $\partial\varphi(x)$. The metric projection of a point $v_1 \in \mathcal{H}$ onto the set C is defined as: $P_C(v_1) = \arg \min_{v_2 \in C} \{\|v_1 - v_2\|\}$. Let \mathcal{H} be a Hilbert space, and

let $v_1, v_2 \in \mathcal{H}$ and $c \in \mathbb{R}$. The following properties hold:

1. $\|v_1 + v_2\|^2 = \|v_1\|^2 + 2\langle v_1, v_2 \rangle + \|v_2\|^2$.
2. $\|v_1 + v_2\|^2 \leq \|v_1\|^2 + 2\langle v_2, v_1 + v_2 \rangle$.
3. $\|cv_1 + (1 - c)v_2\|^2 = c\|v_1\|^2 + (1 - c)\|v_2\|^2 - c(1 - c)\|v_1 - v_2\|^2$.

Definition 2.1 ([35]). Let $\mathcal{B} : \mathcal{H} \times \mathcal{H} \rightarrow \mathbb{R}$ be a bifunction on the set C and $\varsigma > 0$ and \mathcal{B} is called:

- (i) *strongly monotone* if $\mathcal{B}(s_1, s_2) + \mathcal{B}(s_2, s_1) \leq -\varsigma\|s_1 - s_2\|^2$, $\forall s_1, s_2 \in C$,
- (ii) *monotone* if $\mathcal{B}(s_1, s_2) + \mathcal{B}(s_2, s_1) \leq 0$, $\forall s_1, s_2 \in C$,
- (iii) *strongly pseudomonotone* if $\mathcal{B}(s_1, s_2) \geq 0 \implies \mathcal{B}(s_2, s_1) \leq -\varsigma\|s_1 - s_2\|^2$, $\forall s_1, s_2 \in C$,
- (iv) *pseudomonotone* if $\mathcal{B}(s_1, s_2) \geq 0 \implies \mathcal{B}(s_2, s_1) \leq 0$, $\forall s_1, s_2 \in C$.

Lemma 2.2 ([36]). Let $\varphi : C \rightarrow \mathbb{R}$ be a lower semicontinuous convex function defined on the set C . A point $x \in C$ is characterized as a minimizer of the function φ if and only if

$$0 \in \partial\varphi(x) + N_C(x),$$

where $\partial\varphi(x)$ denotes the subdifferential of φ at the point x , and $N_C(x)$ represents the normal cone to the set C at the point x .

Lemma 2.3 ([15]). Let $\{a_k\} \subset [0, +\infty)$, $\{b_k\} \subset (0, 1)$, and $\{c_k\} \subset \mathbb{R}$ be sequences that satisfy the following conditions:

$$a_{k+1} \leq (1 - b_k)a_k + b_k c_k, \quad \forall k \in \mathbb{N},$$

and $\sum_{k=1}^{+\infty} b_k = +\infty$. If for every subsequence $\{a_{k_j}\}$ of $\{a_k\}$, the following conditions hold:

$$\limsup_{j \rightarrow +\infty} c_{k_j} \leq 0 \quad \text{and} \quad \liminf_{j \rightarrow +\infty} (a_{k_j+1} - a_{k_j}) \geq 0,$$

then it follows that $\lim_{k \rightarrow +\infty} a_k = 0$.

Lemma 2.4 ([37]). Let $\{a_k\}$ and $\{b_k\}$ denote sequences of non-negative real numbers. If for all $k \in \mathbb{N}$, $a_{k+1} \leq a_k + b_k$ and $\sum_{k=1}^{+\infty} b_k < +\infty$, then $\lim_{k \rightarrow +\infty} a_k$ exists.

Lemma 2.5 ([38]). Let \mathcal{H} be a real Hilbert space and let $\{x_k\}$ be a sequence in \mathcal{H} . Assume that there exists a nonempty closed set $C \subset \mathcal{H}$ such that:

- (i) For every $z \in C$, $\lim_{k \rightarrow \infty} \|x_k - z\|$ exists.
- (ii) Every weak cluster point of the sequence $\{x_k\}$ is contained in the set C .

Then, there exists an element $\bar{z} \in C$ such that the sequence $\{x_k\}$ converges weakly to \bar{z} .

3. Main results

This section presents two new relaxed inertial subgradient extragradient algorithms aimed at addressing the (EP). Both algorithms utilize adaptive step-size strategies. The proposed methods are based on the subgradient extragradient algorithm, the inertial method, the relaxation technique, and an adaptive step size strategy. Under appropriate conditions, the proposed algorithms are proven to have weak convergence and strong convergence, respectively. A comprehensive, step-by-step description of the first algorithm is provided below:

Assumption 3.1. In order to establish both weak and strong convergence theorems, we consider the following conditions:

- (F1) The solution set of problem (EP), denoted by $\text{EP}(C, \mathcal{B})$, is nonempty.
- (F2) The bifunction \mathcal{B} is pseudomonotone.
- (F3) The bifunction \mathcal{B} satisfies a Lipschitz-type condition as defined in (L-type).
- (F4) For each fixed $s_1 \in \mathcal{H}$, the function $\mathcal{B}(s_1, \cdot)$ is convex on \mathcal{H} .
- (F5) For any sequence $\{y_k\} \subset C$ that converges weakly to y^* , the following inequality holds:

$$\limsup_{k \rightarrow +\infty} \mathcal{B}(y_k, s_1) \leq \mathcal{B}(y^*, s_1), \quad \forall s_1 \in C.$$

To support our analysis, we examine the sequence $\{\varpi_k\}$, which is essential for establishing convergence in our iterative scheme. This sequence influences the step sizes, thereby ensuring both stability and efficacy. The subsequent lemma demonstrates that $\{\varpi_k\}$ is well-defined.

Lemma 3.2 ([26, Lemma 3.1]). Let $\{\varpi_k\}$ be defined by (3). Then $\{\varpi_k\}$ converging to ϖ .

Algorithm 1 : Weakly Convergent Relaxed Inertial Extragradient Method

- 1: Initialization: Set $x_0, x_1 \in \mathcal{H}$, $\theta \in [0, 1]$, $\varpi_1 > 0$, $\kappa \in (0, 1)$, $\tau \in (0, 1)$, and $\mu \in (0, 1)$.
- 2: Select a positive sequence $\{\epsilon_k\}$ that satisfies $\sum_{k=1}^{\infty} \epsilon_k < \infty$.
- 3: Iterations: For each k , perform the following steps:
- 4: Compute θ_k as:

$$0 \leq \theta_k \leq \hat{\theta}_k = \min \left\{ \frac{\theta}{2}, \frac{\epsilon_k}{\|x_k - x_{k-1}\|} \right\} \quad \text{if } x_k \neq x_{k-1}, \quad \text{otherwise} \quad \hat{\theta}_k = \frac{\theta}{2}. \quad (2)$$

- 5: Set $w_k = x_k + \theta_k(x_k - x_{k-1})$.
- 6: Compute $y_k = \arg \min_{y \in \mathcal{C}} \left\{ \varpi_k \mathcal{B}(w_k, y) + \frac{1}{2} \|w_k - y\|^2 \right\}$.
- 7: Determine z_k by finding $\omega_k \in \partial_2 \mathcal{B}(w_k, y_k)$ such that $w_k - \varpi_k \omega_k - y_k \in N_{\mathcal{C}}(y_k)$, and let

$$\mathcal{H}_k = \{z \in \mathcal{H} : \langle w_k - \varpi_k \omega_k - y_k, z - y_k \rangle \leq 0\}.$$

- Then, compute $z_k = \arg \min_{y \in \mathcal{H}_k} \left\{ \kappa \varpi_k \mathcal{B}(y_k, y) + \frac{1}{2} \|w_k - y\|^2 \right\}$.
- 8: Update $x_{k+1} = (1 - \tau)w_k + \tau z_k$.
 - 9: Adjust the step size ϖ_{k+1} according to the rule:

$$\varpi_{k+1} = \begin{cases} \min \left\{ \varpi_k, \frac{\mu}{2} \frac{[\|w_k - y_k\|^2 + \|z_k - y_k\|^2]}{\mathcal{B}(w_k, z_k) - \mathcal{B}(w_k, y_k) - \mathcal{B}(y_k, z_k)} \right\} & \text{if } \mathcal{B}(w_k, z_k) - \mathcal{B}(w_k, y_k) - \mathcal{B}(y_k, z_k) > 0, \\ \varpi_k, & \text{otherwise.} \end{cases} \quad (3)$$

- 10: Set $k := k + 1$, and again conduct the above process.

Remark 3.3. The following property is essential for the analysis of the convergence behavior of the algorithm.

- When the parameters $\theta = 0$ and $\kappa = 1$, the algorithm simplifies to the standard relaxed extragradient method, as delineated in [8].
- By integrating the expression in equation (2) with the constraint $0 \leq \theta_k \leq \hat{\theta}_k$, we derive the inequality:

$$\theta_k \|x_k - x_{k-1}\| \leq \hat{\theta}_k \|x_k - x_{k-1}\| \leq \epsilon_k.$$

This combining with $\sum_{k=1}^{\infty} \epsilon_k < \infty$ implies that $\sum_{k=1}^{\infty} \theta_k \|x_k - x_{k-1}\| < \infty$. As ϵ_k approaches zero as $k \rightarrow \infty$, we obtain

$$\lim_{k \rightarrow +\infty} \theta_k \|x_k - x_{k-1}\| \leq \lim_{k \rightarrow +\infty} \epsilon_k = 0.$$

Consequently, the sequence $\{\theta_k \|x_k - x_{k-1}\|\}$ is bounded.

To demonstrate the convergence of the sequence generated by Algorithm 1, we will establish a crucial inequality in the subsequent lemma that constrains the distance between each iterate z_k and the solution x^* in terms of the previous iterates w_k and y_k .

Lemma 3.4. Let $\{x_k\}$ be a sequence generated by Algorithm 1 with the step size rule (3), satisfying Assumption 3.1. Let x^* be an arbitrary solution to the equilibrium problem. Then, the following inequality holds:

$$\|z_k - x^*\|^2 \leq \|w_k - x^*\|^2 - (1 - \kappa) \|z_k - w_k\|^2 - \left(1 - \frac{\mu \varpi_k}{\varpi_{k+1}}\right) (\|w_k - y_k\|^2 + \|z_k - y_k\|^2).$$

Proof. Using the definition of z_k from Algorithm 1 and applying Lemma 2.2, we have

$$0 \in \partial_2 \left\{ \kappa \varpi_k \mathcal{B}(y_k, \cdot) + \frac{1}{2} \|w_k - \cdot\|^2 \right\} (z_k) + N_{\mathcal{H}_k}(z_k).$$

If $v \in \partial \mathcal{B}(y_k, z_k)$, then there exists a vector $\bar{v} \in N_{\mathcal{H}_k}(z_k)$ such that: $\kappa \varpi_k v + z_k - w_k + \bar{v} = 0$. Thus, we have the following relation

$$\langle w_k - z_k, y - z_k \rangle = \kappa \varpi_k \langle v, y - z_k \rangle + \langle \bar{v}, y - z_k \rangle.$$

Since $\bar{v} \in N_{\mathcal{H}_k}(z_k)$, it follows that $\langle \bar{v}, y - z_k \rangle \leq 0$. Hence,

$$\langle w_k - z_k, y - z_k \rangle \leq \kappa \varpi_k \langle v, y - z_k \rangle. \quad (4)$$

Moreover, since $v \in \partial \mathcal{B}(y_k, z_k)$, we have

$$\mathcal{B}(y_k, y) - \mathcal{B}(y_k, z_k) \geq \langle v, y - z_k \rangle, \quad \forall y \in \mathcal{H}. \quad (5)$$

Combining (4) and (5), we obtain

$$\kappa \varpi_k [\mathcal{B}(y_k, y) - \mathcal{B}(y_k, z_k)] \geq \langle w_k - z_k, y - z_k \rangle, \quad \forall y \in \mathcal{H}_k. \quad (6)$$

Since $z_k \in \mathcal{H}_k$, it holds that

$$\langle w_k - y_k, z_k - y_k \rangle \leq \varpi_k \langle \omega_k, z_k - y_k \rangle. \quad (7)$$

By the definition of the subdifferential, for any $y \in \mathcal{H}_k$, we arrive at

$$\mathcal{B}(w_k, z_k) - \mathcal{B}(w_k, y_k) \geq \langle \omega_k, z_k - y_k \rangle. \quad (8)$$

Combining (7) and (8), we obtain

$$\varpi_k \{ \mathcal{B}(w_k, z_k) - \mathcal{B}(w_k, y_k) \} \geq \langle w_k - y_k, z_k - y_k \rangle. \quad (9)$$

Given that $x^* \in \text{EP}(\mathcal{C}, \mathcal{B})$, substituting $y = x^*$ into expression (6) gives

$$\kappa \varpi_k \mathcal{B}(y_k, x^*) - \kappa \varpi_k \mathcal{B}(y_k, z_k) \geq \langle w_k - z_k, x^* - z_k \rangle.$$

Using condition (F2), we can simplify this further to the following:

$$\langle w_k - z_k, z_k - x^* \rangle \geq \kappa \varpi_k \mathcal{B}(y_k, z_k). \quad (10)$$

From expression (2), we have the inequality

$$\mathcal{B}(w_k, z_k) - \mathcal{B}(w_k, y_k) - \mathcal{B}(y_k, z_k) \leq \frac{\mu (\|w_k - y_k\|^2 + \|z_k - y_k\|^2)}{2\varpi_{k+1}}.$$

Multiplying both sides by $\varpi_k > 0$, we obtain

$$\varpi_k \mathcal{B}(y_k, z_k) \geq \varpi_k \mathcal{B}(w_k, z_k) - \varpi_k \mathcal{B}(w_k, y_k) - \frac{\varpi_k \mu (\|w_k - y_k\|^2 + \|z_k - y_k\|^2)}{2\varpi_{k+1}}. \quad (11)$$

The combination of inequalities (9) and (10) gives

$$\frac{1}{\kappa} \langle w_k - z_k, z_k - x^* \rangle \geq \langle w_k - y_k, z_k - y_k \rangle - \frac{\varpi_k \mu (\|w_k - y_k\|^2 + \|z_k - y_k\|^2)}{2\varpi_{k+1}}.$$

Now, using the identity

$$2\langle w_k - z_k, z_k - x^* \rangle = \|w_k - x^*\|^2 - \|z_k - w_k\|^2 - \|z_k - x^*\|^2,$$

and the identity

$$2\langle y_k - w_k, y_k - z_k \rangle = \|w_k - y_k\|^2 + \|z_k - y_k\|^2 - \|w_k - z_k\|^2,$$

we can derive the following inequality

$$\begin{aligned} \|z_k - x^*\|^2 &\leq \|w_k - x^*\|^2 - (1 - \kappa) \|z_k - w_k\|^2 - \|w_k - y_k\|^2 \\ &\quad - \|z_k - y_k\|^2 + \frac{\varpi_k \mu (\|w_k - y_k\|^2 + \|z_k - y_k\|^2)}{\varpi_{k+1}}. \end{aligned}$$

Alternatively, this can be written as:

$$\|z_k - x^*\|^2 \leq \|w_k - x^*\|^2 - (1 - \kappa) \|z_k - w_k\|^2 - \left(1 - \frac{\mu \varpi_k}{\varpi_{k+1}}\right) (\|w_k - y_k\|^2 + \|z_k - y_k\|^2).$$

This completes the proof. \square

We now present a main theorem that establishes the weak convergence of the sequence $\{x_k\}$ generated by Algorithm 1 to a solution of the equilibrium problem.

Theorem 3.5. *Let $\mathcal{B} : \mathcal{C} \times \mathcal{C} \rightarrow \mathbb{R}$ satisfy Assumption 3.1. Then, the sequence $\{x_k\}$ generated by Algorithm 1 converges weakly to some point $x^* \in \text{EP}(\mathcal{C}, \mathcal{B})$, where x^* is the solutions to the equilibrium problem.*

Proof. By the definition of x_{k+1} , we have

$$\|x_{k+1} - x^*\| = \|(1 - \tau)w_k + \tau z_k - x^*\| = \|(1 - \tau)(w_k - x^*) + \tau(z_k - x^*)\|.$$

Using the convexity of the norm, this implies

$$\|x_{k+1} - x^*\| \leq (1 - \tau)\|w_k - x^*\| + \tau\|z_k - x^*\|. \quad (12)$$

From the definition of w_k in the algorithm, we find

$$\|w_k - x^*\| \leq \|x_k - x^*\| + \theta_k \|x_k - x_{k-1}\|. \quad (13)$$

Applying [Lemma 3.2](#), we obtain

$$\lim_{k \rightarrow +\infty} \left(1 - \frac{\mu \varpi_k}{\varpi_{k+1}} \right) = 1 - \mu > 0,$$

which ensures the existence of $N_1 \in \mathbb{N}$ such that

$$\left(1 - \frac{\mu \varpi_k}{\varpi_{k+1}} \right) > 0, \quad \forall k \geq N_1.$$

Using [Lemma 3.4](#), we also obtain

$$\|z_k - x^*\|^2 \leq \|w_k - x^*\|^2,$$

which implies that

$$\|z_k - x^*\| \leq \|x_k - x^*\| + \theta_k \|x_k - x_{k-1}\|. \quad (14)$$

Substituting (13) and (14) into (12) gives

$$\begin{aligned} \|x_{k+1} - x^*\| &\leq (1 - \tau) (\|x_k - x^*\| + \theta_k \|x_k - x_{k-1}\|) + \tau (\|x_k - x^*\| + \theta_k \|x_k - x_{k-1}\|) \\ &= \|x_k - x^*\| + \theta_k \|x_k - x_{k-1}\|. \end{aligned}$$

Finally, applying [Lemma 2.4](#) with $a_k := \|x_k - x^*\|$ and $b_k := \theta_k \|x_k - x_{k-1}\|$, we conclude that

$$\lim_{k \rightarrow \infty} \|x_k - x^*\|$$

exists, proving that the sequence $\{x_k\}$ is bounded. Using (13), we obtain

$$\begin{aligned} \|w_k - x^*\|^2 &\leq (\|x_k - x^*\| + K_1)^2 \\ &= \|x_k - x^*\|^2 + 2K_1 \|x_k - x^*\| + K_1^2 \\ &\leq \|x_k - x^*\|^2 + K_2, \end{aligned} \quad (15)$$

where K_1 is an upper bound for the inertial term $\theta_k \|x_k - x_{k-1}\|$ and K_2 is a positive constant such that $K_2 > 0$. From [Lemma 3.4](#), we also have

$$\begin{aligned} \|z_k - x^*\|^2 &\leq \|w_k - x^*\|^2 - (1 - \kappa) \|w_k - z_k\|^2 \\ &\quad - \left(1 - \frac{\mu \varpi_k}{\varpi_{k+1}} \right) \|w_k - y_k\|^2 - \left(1 - \frac{\mu \varpi_k}{\varpi_{k+1}} \right) \|z_k - y_k\|^2. \end{aligned} \quad (16)$$

Combining (15) and (16), we derive

$$\begin{aligned} \|z_k - x^*\|^2 &\leq \|x_k - x^*\|^2 + K_2 - (1 - \kappa) \|w_k - z_k\|^2 \\ &\quad - \left(1 - \frac{\mu \varpi_k}{\varpi_{k+1}} \right) \|w_k - y_k\|^2 - \left(1 - \frac{\mu \varpi_k}{\varpi_{k+1}} \right) \|z_k - y_k\|^2. \end{aligned} \quad (17)$$

To simplify the expression for $\|x_{k+1} - x^*\|^2$, we proceed as follows

$$\begin{aligned} \|x_{k+1} - x^*\|^2 &= \|(1 - \tau) w_k + \tau z_k - x^*\|^2 \\ &= \left\| (1 - \tau) [w_k - x^*] + \tau [z_k - x^*] \right\|^2 \\ &= (1 - \tau) \|w_k - x^*\|^2 + \tau \|z_k - x^*\|^2 - \tau(1 - \tau) \|z_k - w_k\|^2 \\ &\leq (1 - \tau) \|w_k - x^*\|^2 + \tau \|z_k - x^*\|^2. \end{aligned} \quad (18)$$

Substituting the inequalities from (15) and (17) into (18), we deduce that

$$\begin{aligned} \|x_{k+1} - x^*\|^2 &\leq (1 - \tau) \|w_k - x^*\|^2 + \tau \|z_k - x^*\|^2 \\ &\leq (1 - \tau) \|x_k - x^*\|^2 + (1 - \tau) K_2 + \tau \|x_k - x^*\|^2 + \tau K_2 \\ &\quad - \tau(1 - \kappa) \|w_k - z_k\|^2 - \tau \left(1 - \frac{\mu \varpi_k}{\varpi_{k+1}} \right) \|w_k - y_k\|^2 \\ &\quad - \tau \left(1 - \frac{\mu \varpi_k}{\varpi_{k+1}} \right) \|z_k - y_k\|^2. \end{aligned}$$

Thus, the expression simplifies to:

$$\begin{aligned} \tau(1 - \kappa) \|w_k - z_k\|^2 &+ \tau \left(1 - \frac{\mu \varpi_k}{\varpi_{k+1}} \right) (\|w_k - y_k\|^2 + \|z_k - y_k\|^2) \\ &\leq \|x_k - x^*\|^2 - \|x_{k+1} - x^*\|^2 + K_2. \end{aligned} \quad (19)$$

Taking the limit in (19) and noting that $\{\|x_k - x^*\|^2\}$ converges to zero as $k \rightarrow \infty$, we obtain

$$\lim_{k \rightarrow +\infty} \|w_k - z_k\| = 0, \quad \lim_{k \rightarrow +\infty} \|w_k - y_k\| = 0, \quad \lim_{k \rightarrow +\infty} \|z_k - y_k\| = 0. \quad (20)$$

By Lemma 2.5, it suffices to show that any weak cluster point of $\{x_k\}$ belongs to the solution set $\text{EP}(C, \mathcal{B})$. Let \hat{x} be an arbitrary weak cluster point of $\{x_k\}$. Since $\{x_k\}$ is bounded, there exists a subsequence $\{x_{k_j}\}$ such that $x_{k_j} \rightharpoonup \hat{x}$. Furthermore, by (20), $y_{k_j} \rightharpoonup \hat{x}$ and $\hat{x} \in C$. Next, we prove that $\hat{x} \in \text{EP}(C, \mathcal{B})$. Using (6), we have

$$\kappa \varpi_{k_j} \mathcal{B}(y_{k_j}, y) \geq \kappa \varpi_{k_j} \mathcal{B}(y_{k_j}, z_{k_j}) + \langle w_{k_j} - z_{k_j}, y - z_{k_j} \rangle, \quad \forall y \in \mathcal{H}_k. \quad (21)$$

Additionally, from (9), we obtain

$$\kappa \varpi_{k_j} (\mathcal{B}(w_{k_j}, z_{k_j}) - \mathcal{B}(w_{k_j}, y_{k_j})) \geq \kappa \langle w_{k_j} - y_{k_j}, z_{k_j} - y_{k_j} \rangle.$$

Moreover, from (11), we have

$$\begin{aligned} \varpi_{k_j} \mathcal{B}(y_{k_j}, z_{k_j}) &\geq \varpi_{k_j} \mathcal{B}(w_{k_j}, z_{k_j}) - \varpi_{k_j} \mathcal{B}(w_{k_j}, y_{k_j}) \\ &\quad - \frac{\varpi_{k_j} \mu (\|w_{k_j} - y_{k_j}\|^2 + \|z_{k_j} - y_{k_j}\|^2)}{2 \varpi_{k_j+1}}. \end{aligned} \quad (22)$$

Combining (21) and (22), we obtain

$$\begin{aligned} \kappa \varpi_{k_j} \mathcal{B}(y_{k_j}, y) &\geq \kappa \varpi_{k_j} \mathcal{B}(w_{k_j}, z_{k_j}) - \kappa \varpi_{k_j} \mathcal{B}(w_{k_j}, y_{k_j}) + \langle w_{k_j} - z_{k_j}, y - z_{k_j} \rangle \\ &\quad - \frac{\varpi_{k_j} \mu \|w_{k_j} - y_{k_j}\|^2}{2 \varpi_{k_j+1}} - \frac{\varpi_{k_j} \mu \|z_{k_j} - y_{k_j}\|^2}{2 \varpi_{k_j+1}}. \end{aligned}$$

By simplifying further using (22), we conclude that

$$\begin{aligned} \kappa \varpi_{k_j} \mathcal{B}(y_{k_j}, y) &\geq \kappa \langle w_{k_j} - y_{k_j}, z_{k_j} - y_{k_j} \rangle + \langle w_{k_j} - z_{k_j}, y - z_{k_j} \rangle \\ &\quad - \frac{\varpi_{k_j} \mu \|w_{k_j} - y_{k_j}\|^2}{2 \varpi_{k_j+1}} - \frac{\varpi_{k_j} \mu \|z_{k_j} - y_{k_j}\|^2}{2 \varpi_{k_j+1}}. \end{aligned}$$

Here, y is an arbitrary element of the set \mathcal{H}_k . From (20), and the boundedness of $\{x_{k_j}\}$, the right-hand side tends to zero. Given $\varpi_{k_j} > 0$, condition (F5), and $y_{k_j} \rightharpoonup \hat{x}$, we deduce:

$$0 \leq \limsup_{j \rightarrow \infty} \mathcal{B}(y_{k_j}, y) \leq \mathcal{B}(\hat{x}, y), \quad \forall y \in \mathcal{H}_k.$$

Thus, $\mathcal{B}(\hat{x}, y) \geq 0$ for all $y \in C$, implying that $\hat{x} \in \text{EP}(C, \mathcal{B})$. Therefore, we have established the following:

1. For every $x^* \in \text{EP}(C, \mathcal{B})$, $\lim_{k \rightarrow \infty} \|x_k - x^*\|^2$ exists;
2. Every weak cluster point of $\{x_k\}$ lies in $\text{EP}(C, \mathcal{B})$.

By Lemma 2.5, the sequence $\{x_k\}$ converges weakly to $x^* \in \text{EP}(C, \mathcal{B})$. \square

Next, we present another relaxed inertial subgradient extragradient algorithm designed to address the equilibrium problem (EP). A comprehensive, step-by-step elucidation of the second algorithm is provided below:

Theorem 3.6. *Let $\mathcal{B} : C \times C \rightarrow \mathbb{R}$ satisfy Assumption 3.1. Then, the sequence $\{x_k\}$ generated by Algorithm 2 converges strongly to an element $x^* \in \text{EP}(C, \mathcal{B})$, where x^* is the projection of the origin onto the set of solutions to the equilibrium problem.*

Proof. We divide the proof into four claims.

Claim 1: The sequence $\{x_k\}$ is bounded.

From (23), we have

$$\lim_{k \rightarrow \infty} \frac{\theta_k}{\beta_k} \|x_k - x_{k-1}\| = \lim_{k \rightarrow \infty} \frac{\epsilon_k}{\beta_k} \|x_k - x_{k-1}\| = 0. \quad (24)$$

Using the definition of $\{w_k\}$ and inequality (24), we have

$$\begin{aligned} \|w_k - x^*\| &= \|x_k + \theta_k(x_k - x_{k-1}) - \beta_k x_k - \theta_k \beta_k(x_k - x_{k-1}) - x^*\| \\ &= \|(1 - \beta_k)(x_k - x^*) + (1 - \beta_k)\theta_k(x_k - x_{k-1}) - \beta_k x^*\| \\ &\leq (1 - \beta_k) \|x_k - x^*\| + (1 - \beta_k)\theta_k \|x_k - x_{k-1}\| + \beta_k \|x^*\| \\ &\leq (1 - \beta_k) \|x_k - x^*\| + \beta_k M_1, \end{aligned} \quad (25)$$

where

$$(1 - \beta_k) \frac{\theta_k}{\beta_k} \|x_k - x_{k-1}\| + \|x^*\| \leq M_1.$$

Algorithm 2 : Strongly Convergent Relaxed Inertial Extragradient Method

- 1: Initialize: Let $x_0, x_1 \in \mathcal{H}$, $\theta \in [0, 1)$, $\varpi_1 > 0$, $\kappa \in (0, 1]$, $\tau \in (0, 1)$, and $\mu \in (0, 1)$.
- 2: Select two positive sequences $\{\beta_k\} \subset (0, 1)$ and $\{\epsilon_k\}$ such that

$$\lim_{k \rightarrow +\infty} \beta_k = 0, \quad \sum_{k=1}^{+\infty} \beta_k = +\infty, \quad \text{and} \quad \lim_{k \rightarrow +\infty} \frac{\epsilon_k}{\beta_k} = 0. \quad (23)$$

- 3: Iterations: For each k , perform the following steps:

- 4: Compute θ_k as

$$0 \leq \theta_k \leq \hat{\theta}_k = \min \left\{ \frac{\theta}{2}, \frac{\epsilon_k}{\|x_k - x_{k-1}\|} \right\} \quad \text{if } x_k \neq x_{k-1}, \quad \text{otherwise} \quad \hat{\theta}_k = \frac{\theta}{2}.$$

- 5: Compute $w_k = (1 - \beta_k) [x_k + \theta_k(x_k - x_{k-1})]$.

- 6: Compute $y_k = \arg \min_{y \in C} \left\{ \varpi_k \mathcal{B}(w_k, y) + \frac{1}{2} \|w_k - y\|^2 \right\}$.

- 7: Compute z_k such that $\omega_k \in \partial_2 \mathcal{B}(w_k, y_k)$ satisfies $w_k - \varpi_k \omega_k - y_k \in N_C(y_k)$, and $\mathcal{H}_k = \{z \in \mathcal{H} : \langle w_k - \varpi_k \omega_k - y_k, z - y_k \rangle \leq 0\}$, then compute

$$z_k = \arg \min_{y \in \mathcal{H}_k} \left\{ \kappa \varpi_k \mathcal{B}(y_k, y) + \frac{1}{2} \|w_k - y\|^2 \right\}.$$

- 8: Compute $x_{k+1} = (1 - \tau)w_k + \tau z_k$.

- 9: Update the step size rule:

$$\varpi_{k+1} = \begin{cases} \min \left\{ \varpi_k, \frac{\mu [\|w_k - y_k\|^2 + \|z_k - y_k\|^2]}{\mathcal{B}(w_k, z_k) - \mathcal{B}(w_k, y_k) - \mathcal{B}(y_k, z_k)} \right\} & \text{if } \mathcal{B}(w_k, z_k) - \mathcal{B}(w_k, y_k) - \mathcal{B}(y_k, z_k) > 0, \\ \varpi_k, & \text{otherwise.} \end{cases}$$

- 10: Set $k := k + 1$, and again conduct the above process.

By applying [Lemma 3.4](#), we obtain

$$\begin{aligned} \|z_k - x^*\|^2 &\leq \|w_k - x^*\|^2 - (1 - \kappa) \|z_k - w_k\|^2 \\ &\quad - \left(1 - \frac{\mu \varpi_k}{\varpi_{k+1}}\right) \|w_k - y_k\|^2 - \left(1 - \frac{\mu \varpi_k}{\varpi_{k+1}}\right) \|z_k - y_k\|^2. \end{aligned} \quad (26)$$

According to [Lemma 3.2](#), we have

$$\lim_{k \rightarrow \infty} \left(1 - \frac{\mu \varpi_k}{\varpi_{k+1}}\right) = 1 - \mu > 0.$$

This implies the existence of a natural number $N_2 \in \mathbb{N}$ such that

$$1 - \frac{\mu \varpi_k}{\varpi_{k+1}} > 0, \quad \forall k \geq N_2.$$

Using (26), we obtain

$$\|z_k - x^*\| \leq \|w_k - x^*\| \leq (1 - \beta_k) \|x_k - x^*\| + \beta_k M_1.$$

By the definition of $\{x_{k+1}\}$, we have

$$\begin{aligned} \|x_{k+1} - x^*\| &= \|(1 - \tau)w_k + \tau z_k - x^*\| \\ &= \|(1 - \tau)[w_k - x^*] + \tau[z_k - x^*]\| \\ &\leq (1 - \tau) \|w_k - x^*\| + \tau \|z_k - x^*\|. \end{aligned}$$

The expression for $(1 - \tau) \|w_k - x^*\|$ is given by

$$\begin{aligned} (1 - \tau) \|w_k - x^*\| &\leq (1 - \tau) ((1 - \beta_k) \|x_k - x^*\| + \beta_k M_1) \\ &= (1 - \tau)(1 - \beta_k) \|x_k - x^*\| + (1 - \tau)\beta_k M_1. \end{aligned}$$

Substituting the bounds for $\|w_k - x^*\|$ and $\|z_k - x^*\|$, we obtain

$$\begin{aligned} \|x_{k+1} - x^*\| &\leq (1 - \tau)(1 - \beta_k) \|x_k - x^*\| + (1 - \tau)\beta_k M_1 \\ &\quad + \tau(1 - \beta_k) \|x_k - x^*\| + \tau\beta_k M_1. \end{aligned}$$

To simplify the coefficients for $\|x_k - x^*\|$, we compute

$$(1 - \tau)(1 - \beta_k) + \tau(1 - \beta_k) = (1 - \beta_k)((1 - \tau) + \tau) = 1 - \beta_k.$$

Similarly, for the coefficients of M_1 , we have

$$(1 - \tau)\beta_k + \tau\beta_k = \beta_k((1 - \tau) + \tau) = \beta_k.$$

Thus, the expression simplifies to

$$\|x_{k+1} - x^*\| \leq (1 - \beta_k)\|x_k - x^*\| + \beta_k M_1.$$

From the above expression, we obtain

$$\begin{aligned} \|x_{k+1} - x^*\| &\leq (1 - \beta_k)\|x_k - x^*\| + \beta_k M_1 \\ &\leq \max \{\|x_k - x^*\|, M_1\} \\ &\vdots \\ &\leq \max \{\|x_0 - x^*\|, M_1\}. \end{aligned}$$

Hence, we conclude that the sequence $\{x_k\}$ is bounded.

Claim 2:

$$\begin{aligned} \tau(1 - \kappa)\|w_k - z_k\|^2 + \tau \left(1 - \frac{\mu\varpi_k}{\varpi_{k+1}}\right) \|w_k - y_k\|^2 + \tau \left(1 - \frac{\mu\varpi_k}{\varpi_{k+1}}\right) \|z_k - y_k\|^2 \\ \leq \|x_k - x^*\|^2 - \|x_{k+1} - x^*\|^2 + \beta_k M_2. \end{aligned}$$

Using (25), we deduce that

$$\begin{aligned} \|w_k - x^*\|^2 &\leq (1 - \beta_k)^2 \|x_k - x^*\|^2 + \beta_k^2 M_1^2 + 2M_1\beta_k(1 - \beta_k)\|x_k - x^*\| \\ &\leq \|x_k - x^*\|^2 + \beta_k [\beta_k M_1^2 + 2M_1(1 - \beta_k)\|x_k - x^*\|] \\ &\leq \|x_k - x^*\|^2 + \beta_k M_2, \end{aligned} \tag{27}$$

where $M_2 > 0$. Furthermore, from Lemma 3.4 and (27), we have

$$\begin{aligned} \|z_k - x^*\|^2 &\leq \|x_k - x^*\|^2 + \beta_k M_2 - (1 - \kappa)\|w_k - z_k\|^2 \\ &\quad - \left(1 - \frac{\mu\varpi_k}{\varpi_{k+1}}\right) \|w_k - y_k\|^2 - \left(1 - \frac{\mu\varpi_k}{\varpi_{k+1}}\right) \|z_k - y_k\|^2. \end{aligned} \tag{28}$$

Given the definition of x_{k+1} , we find

$$\begin{aligned} \|x_{k+1} - x^*\|^2 &= \|(1 - \tau)w_k + \tau z_k - x^*\|^2 \\ &= \|(1 - \tau)[w_k - x^*] + \tau[z_k - x^*]\|^2 \\ &= (1 - \tau)\|w_k - x^*\|^2 + \tau\|z_k - x^*\|^2 - \tau(1 - \tau)\|z_k - w_k\|^2 \\ &\leq (1 - \tau)\|w_k - x^*\|^2 + \tau\|z_k - x^*\|^2. \end{aligned} \tag{29}$$

To simplify $\|x_{k+1} - x^*\|^2$, we substitute $\|w_k - x^*\|^2$ from (27) and $\|z_k - x^*\|^2$ from (28) into (29), we obtain

$$\begin{aligned} \|x_{k+1} - x^*\|^2 &\leq (1 - \tau)\|w_k - x^*\|^2 + \tau\|z_k - x^*\|^2 \\ &\leq (1 - \tau)\|x_k - x^*\|^2 + (1 - \tau)\beta_k M_2 + \tau\|x_k - x^*\|^2 + \tau\beta_k M_2 \\ &\quad - \tau(1 - \kappa)\|w_k - z_k\|^2 - \tau \left(1 - \frac{\mu\varpi_k}{\varpi_{k+1}}\right) (\|w_k - y_k\|^2 + \|z_k - y_k\|^2). \end{aligned}$$

Thus, the final expression is:

$$\begin{aligned} \tau(1 - \kappa)\|w_k - z_k\|^2 + \tau \left(1 - \frac{\mu\varpi_k}{\varpi_{k+1}}\right) \|w_k - y_k\|^2 + \tau \left(1 - \frac{\mu\varpi_k}{\varpi_{k+1}}\right) \|z_k - y_k\|^2 \\ \leq \|x_k - x^*\|^2 - \|x_{k+1} - x^*\|^2 + \beta_k M_2. \end{aligned}$$

Claim 3:

$$\begin{aligned} \|x_{k+1} - x^*\|^2 &\leq (1 - \beta_k)\|x_k - x^*\|^2 + \beta_k \left[\theta_k \|x_k - x_{k-1}\| + \frac{\theta_k}{\beta_k} \|x_k - x_{k-1}\| \right. \\ &\quad \left. + 2(1 - \beta_k)\|x_k - x^*\| \frac{\theta_k}{\beta_k} \|x_k - x_{k-1}\| \right. \\ &\quad \left. + 2\|x^*\|\|w_k - x_{k+1}\| + 2\langle x^*, x^* - x_{k+1} \rangle \right]. \end{aligned}$$

Using the value of $\{w_k\}$, we have

$$\begin{aligned} \|w_k - x^*\|^2 &= \|x_k + \theta_k(x_k - x_{k-1}) - \beta_k x_k - \theta_k \beta_k(x_k - x_{k-1}) - x^*\|^2 \\ &= \|(1 - \beta_k)(x_k - x^*) + (1 - \beta_k)\theta_k(x_k - x_{k-1}) - \beta_k x^*\|^2 \\ &\leq \|(1 - \beta_k)(x_k - x^*) + (1 - \beta_k)\theta_k(x_k - x_{k-1})\|^2 \end{aligned}$$

$$\begin{aligned}
& + 2\beta_k \langle -x^*, w_k - x^* \rangle \\
& = (1 - \beta_k)^2 \|x_k - x^*\|^2 + (1 - \beta_k)^2 \theta_k^2 \|x_k - x_{k-1}\|^2 \\
& \quad + 2\theta_k(1 - \beta_k)^2 \|x_k - x^*\| \|x_k - x_{k-1}\| + 2\beta_k \langle -x^*, w_k - x_{k+1} \rangle \\
& \quad + 2\beta_k \langle -x^*, x_{k+1} - x^* \rangle \\
& \leq (1 - \beta_k) \|x_k - x^*\|^2 + \theta_k^2 \|x_k - x_{k-1}\|^2 + 2\theta_k(1 - \beta_k) \|x_k - x^*\| \|x_k - x_{k-1}\| \\
& \quad + 2\beta_k \|x^*\| \|w_k - x_{k+1}\| + 2\beta_k \langle x^*, x^* - x_{k+1} \rangle \\
& = (1 - \beta_k) \|x_k - x^*\|^2 + \beta_k \left[\theta_k \|x_k - x_{k-1}\| + \frac{\theta_k}{\beta_k} \|x_k - x_{k-1}\| \right. \\
& \quad \left. + 2(1 - \beta_k) \|x_k - x^*\| \frac{\theta_k}{\beta_k} \|x_k - x_{k-1}\| \right. \\
& \quad \left. + 2\|x^*\| \|w_k - x_{k+1}\| + 2\langle x^*, x^* - x_{k+1} \rangle \right]. \tag{30}
\end{aligned}$$

By applying expression (29), we obtain

$$\|x_{k+1} - x^*\|^2 \leq (1 - \tau) \|w_k - x^*\|^2 + \tau \|z_k - x^*\|^2. \tag{31}$$

Using expressions (30), (31), and the inequality $\|z_k - x^*\| \leq \|w_k - x^*\|$, we derive that the required inequality.

Claim 4: The sequence $\|x_k - x^*\|$ converges to zero.

Note that

$$\begin{aligned}
& \|x_{k+1} - x^*\|^2 \leq (1 - \beta_k) \|x_k - x^*\|^2 + \beta_k \left[\theta_k \|x_k - x_{k-1}\| + \frac{\theta_k}{\beta_k} \|x_k - x_{k-1}\| \right. \\
& \quad \left. + 2(1 - \beta_k) \|x_k - x^*\| \frac{\theta_k}{\beta_k} \|x_k - x_{k-1}\| + 2\|x^*\| \|w_k - x_{k+1}\| + 2\langle x^*, x^* - x_{k+1} \rangle \right].
\end{aligned}$$

Now, define

$$a_k := \|x_k - x^*\|^2$$

and

$$\begin{aligned}
c_k := & \theta_k \|x_k - x_{k-1}\| + \frac{\theta_k}{\beta_k} \|x_k - x_{k-1}\| + 2(1 - \beta_k) \|x_k - x^*\| \frac{\theta_k}{\beta_k} \|x_k - x_{k-1}\| \\
& + 2\|x^*\| \|w_k - x_{k+1}\| + 2\langle x^*, x^* - x_{k+1} \rangle.
\end{aligned}$$

Thus, Claim 4 can be restated as follows:

$$a_{k+1} \leq (1 - \beta_k) a_k + \beta_k c_k.$$

According to Lemma 2.3, it suffices to show that

$$\limsup_{j \rightarrow +\infty} c_{k_j} \leq 0$$

for every subsequence $\{a_{k_j}\}$ of $\{a_k\}$ that satisfies

$$\liminf_{j \rightarrow +\infty} (a_{k_j+1} - a_{k_j}) \geq 0.$$

This is equivalent to demonstrating that

$$\limsup_{j \rightarrow +\infty} \langle x^*, x^* - x_{k_j+1} \rangle \leq 0$$

for every subsequence $\{\|x_{k_j} - x^*\|\}$ of $\{\|x_k - x^*\|\}$ that satisfies

$$\liminf_{j \rightarrow +\infty} (\|x_{k_j+1} - x^*\| - \|x_{k_j} - x^*\|) \geq 0.$$

Assume that $\{\|x_{k_j} - x^*\|\}$ is a subsequence of $\{\|x_k - x^*\|\}$ satisfying

$$\liminf_{j \rightarrow +\infty} (\|x_{k_j+1} - x^*\| - \|x_{k_j} - x^*\|) \geq 0.$$

Then we have

$$\begin{aligned}
& \liminf_{j \rightarrow +\infty} (\|x_{k_j+1} - x^*\|^2 - \|x_{k_j} - x^*\|^2) \\
& = \liminf_{j \rightarrow +\infty} (\|x_{k_j+1} - x^*\| - \|x_{k_j} - x^*\|) (\|x_{k_j+1} - x^*\| + \|x_{k_j} - x^*\|) \geq 0.
\end{aligned}$$

It follows from Claim 2 that

$$\begin{aligned} & \limsup_{j \rightarrow +\infty} \left[\tau(1-\kappa) \|w_{k_j} - z_{k_j}\|^2 + \tau \left(1 - \frac{\mu \varpi_{k_j}}{\varpi_{k_j+1}} \right) \left(\|w_{k_j} - y_{k_j}\|^2 + \|z_{k_j} - y_{k_j}\|^2 \right) \right] \\ & \leq \limsup_{j \rightarrow +\infty} \left[\|x_{k_j} - x^*\|^2 - \|x_{k_j+1} - x^*\|^2 + \beta_{k_j} M_2 \right] \\ & = -\liminf_{j \rightarrow +\infty} \left[\|x_{k_j+1} - x^*\|^2 - \|x_{k_j} - x^*\|^2 \right] \\ & \leq 0. \end{aligned}$$

This implies that

$$\lim_{j \rightarrow +\infty} \|w_{k_j} - z_{k_j}\| = 0, \quad \lim_{j \rightarrow +\infty} \|w_{k_j} - y_{k_j}\| = 0, \quad \lim_{j \rightarrow +\infty} \|z_{k_j} - y_{k_j}\| = 0. \quad (32)$$

Moreover, the following relationship is established:

$$\begin{aligned} \|w_{k_j} - x_{k_j}\| &= \|x_{k_j} + \theta_{k_j}(x_{k_j} - x_{k_j-1}) - \beta_{k_j} [\theta_{k_j}(x_{k_j} - x_{k_j-1})] - x_{k_j}\| \\ &\leq \theta_{k_j} \|x_{k_j} - x_{k_j-1}\| + \beta_{k_j} \|x_{k_j}\| + \theta_{k_j} \beta_{k_j} \|x_{k_j} - x_{k_j-1}\| \\ &= \beta_{k_j} \frac{\theta_{k_j}}{\beta_{k_j}} \|x_{k_j} - x_{k_j-1}\| + \beta_{k_j} \|x_{k_j}\| + \beta_{k_j}^2 \frac{\theta_{k_j}}{\beta_{k_j}} \|x_{k_j} - x_{k_j-1}\| \longrightarrow 0. \end{aligned} \quad (33)$$

The convergence $\|z_{k_j} - w_{k_j}\| \rightarrow 0$ implies that

$$\lim_{j \rightarrow +\infty} \|z_{k_j} - x_{k_j}\| = 0.$$

Given the recurrence relation

$$x_{k+1} = (1-\tau)w_k + \tau z_k,$$

for some $\tau \in (0, 1)$, we can express x_{k_j+1} in terms of w_{k_j} and z_{k_j} as follows:

$$\|w_{k_j} - x_{k_j+1}\| = \left\| w_{k_j} - \left[(1-\tau)w_{k_j} + \tau z_{k_j} \right] \right\| = \left\| \tau(w_{k_j} - z_{k_j}) \right\| = \tau \|w_{k_j} - z_{k_j}\|.$$

Since it is given that $\lim_{j \rightarrow \infty} \|w_{k_j} - z_{k_j}\| = 0$, by the properties of limits, we conclude that

$$\lim_{j \rightarrow \infty} \|w_{k_j} - x_{k_j+1}\| = \tau \cdot 0 = 0.$$

Using the definition $x_{k_j+1} = (1-\tau)w_{k_j} + \tau z_{k_j}$, we have

$$\|x_{k_j} - x_{k_j+1}\| = \left\| x_{k_j} - \left[(1-\tau)w_{k_j} + \tau z_{k_j} \right] \right\|.$$

By applying the triangle inequality, we obtain

$$\|x_{k_j} - x_{k_j+1}\| \leq \|x_{k_j} - w_{k_j}\| + \tau \|w_{k_j} - z_{k_j}\|.$$

Since $\lim_{j \rightarrow \infty} \|x_{k_j} - w_{k_j}\| = 0$ and $\lim_{j \rightarrow \infty} \|w_{k_j} - z_{k_j}\| = 0$, it follows that

$$\lim_{j \rightarrow \infty} \|x_{k_j} - x_{k_j+1}\| = 0 + \tau \cdot 0 = 0.$$

Next, since the sequence $\{x_k\}$ is bounded, there exists a subsequence $\{x_{k_j}\}$ of $\{x_k\}$ such that $x_{k_j} \rightharpoonup \hat{x}$. From expression (33), it follows that $\{w_{k_j}\}$ weakly converges to $\hat{x} \in \mathcal{H}$. Our next goal is to prove that $\hat{x} \in EP(C, \mathcal{B})$. Using expression (6), we obtain the inequality

$$\kappa \varpi_{k_j} \mathcal{B}(y_{k_j}, y) \geq \kappa \varpi_{k_j} \mathcal{B}(y_{k_j}, z_{k_j}) + \langle w_{k_j} - z_{k_j}, y - z_{k_j} \rangle, \quad \forall y \in \mathcal{H}_k. \quad (34)$$

Additionally, from (9), we have

$$\kappa \varpi_{k_j} \{ \mathcal{B}(w_{k_j}, z_{k_j}) - \mathcal{B}(w_{k_j}, y_{k_j}) \} \geq \kappa \langle w_{k_j} - y_{k_j}, z_{k_j} - y_{k_j} \rangle.$$

Moreover, from (11), we obtain the following inequality:

$$\begin{aligned} \varpi_{k_j} \mathcal{B}(y_{k_j}, z_{k_j}) &\geq \varpi_{k_j} \mathcal{B}(w_{k_j}, z_{k_j}) - \varpi_{k_j} \mathcal{B}(w_{k_j}, y_{k_j}) \\ &\quad - \frac{\varpi_{k_j} \mu (\|w_{k_j} - y_{k_j}\|^2 + \|z_{k_j} - y_{k_j}\|^2)}{2 \varpi_{k_{j+1}}}. \end{aligned} \quad (35)$$

Combining expressions (34) and (35), we obtain

$$\kappa \varpi_{k_j} \mathcal{B}(y_{k_j}, y) \geq \kappa \varpi_{k_j} \mathcal{B}(w_{k_j}, z_{k_j}) - \kappa \varpi_{k_j} \mathcal{B}(w_{k_j}, y_{k_j}) + \langle w_{k_j} - z_{k_j}, y - z_{k_j} \rangle$$

$$-\frac{\varpi_{k_j}\mu\|w_{k_j}-y_{k_j}\|^2}{2\varpi_{k_{j+1}}}-\frac{\varpi_{k_j}\mu\|z_{k_j}-y_{k_j}\|^2}{2\varpi_{k_{j+1}}}.$$

By further simplification using (35), we find that

$$\begin{aligned} \kappa\varpi_{k_j}\mathcal{B}(y_{k_j}, y) &\geq \kappa\langle w_{k_j} - y_{k_j}, z_{k_j} - y_{k_j} \rangle + \langle w_{k_j} - z_{k_j}, y - z_{k_j} \rangle \\ &\quad - \frac{\varpi_{k_j}\mu\|w_{k_j}-y_{k_j}\|^2}{2\varpi_{k_{j+1}}}-\frac{\varpi_{k_j}\mu\|z_{k_j}-y_{k_j}\|^2}{2\varpi_{k_{j+1}}}. \end{aligned}$$

Here, y is an arbitrary element of the set \mathcal{H}_k . From expressions (32) and the boundedness of $\{x_{k_j}\}$, the right-hand side approaches zero. Given that $\varpi_{k_j} > 0$, condition (F5), and $y_{k_j} \rightharpoonup \hat{x}$, we conclude that

$$0 \leq \limsup_{j \rightarrow \infty} \mathcal{B}(y_{k_j}, y) \leq \mathcal{B}(\hat{x}, y), \quad \forall y \in \mathcal{H}_k.$$

This implies that $\mathcal{B}(\hat{x}, y) \geq 0$ for all $y \in \mathcal{C}$, and hence $\hat{x} \in \text{EP}(\mathcal{C}, \mathcal{B})$. Next, we have

$$\limsup_{k \rightarrow \infty} \langle x^*, x^* - x_k \rangle = \lim_{j \rightarrow +\infty} \langle x^*, x^* - x_{k_j} \rangle = \langle x^*, x^* - \hat{x} \rangle \leq 0. \quad (36)$$

Using the fact that $\lim_{k \rightarrow \infty} \|x_{k+1} - x_k\| = 0$, we deduce from (36) that

$$\begin{aligned} \limsup_{k \rightarrow \infty} \langle x^*, x^* - x_{k+1} \rangle &\leq \limsup_{k \rightarrow \infty} \langle x^*, x^* - x_k \rangle + \limsup_{k \rightarrow \infty} \langle x^*, x_k - x_{k+1} \rangle \\ &\leq 0. \end{aligned}$$

Combining Claim 3 with Lemma 2.3, we observe that $x_k \rightarrow x^*$ as $k \rightarrow +\infty$. Thus, the proof of Theorem 3.6 is completed. \square

4. Numerical experiments

In this section, we present some computational experiments to assess and compare the performance of the methodologies presented in Section 3 with other related algorithms. Additionally, we investigate and analyze the influence of varying control parameters on their numerical efficiency of the proposed methods. Our experiments were conducted using MATLAB R2022b on a Lenovo laptop equipped with a Core i9-13900H 2.60 GHz processor and 32 GB of RAM. All comparative experiments were carried out under the following parameter settings:

1. For Algorithm 3.1 in [17] (in short iPEGM), we set $\varpi = \frac{1}{10c_1}$, $\theta = 0.12$, $D_k = \max\{\|x_{k+1} - y_k\|, \|x_{k+1} - w_k\|\}$.
2. For Algorithm 2 in [19] (in short iSEGM), we choose $\varpi_1 = 0.60$, $\alpha_k = 0.20$, $\mu = 0.20$, $D_k = \|w_k - y_k\|$.
3. For Algorithm 1 in [18] (in short iEGM), we select $\varpi = \frac{1}{4c_1}$, $\theta = 0.60$, $\epsilon_k = \frac{1}{k^2}$, $D_k = \|w_k - y_k\|$.
4. For Algorithm 1 (in short iREGM), we pick $\varpi_1 = 0.65$, $\theta = 0.60$, $\mu = 0.44$, $\kappa = 0.75$, $\tau = 0.75$, $\epsilon_k = \frac{1}{k^2}$, $D_k = \|w_k - y_k\|^2$.
5. For Algorithm 3 in [18] (in short iMEGM), we select $\varpi = \frac{1}{\max\{4c_1, 4c_2\}}$, $\theta = 0.60$, $\epsilon_k = \frac{1}{k^2}$, $\gamma_k = \frac{1}{5(k+2)}$, $\beta_k = \frac{5}{10}(1 - \gamma_k)$, $D_k = \|w_k - y_k\|^2$.
6. For Algorithm 3.1 in [24] (in short iSMEGM), we set $\varpi_1 = 0.60$, $\theta = 0.60$, $\mu = 0.33$, $\epsilon_k = \frac{1}{k^2}$, $\beta_k = \frac{1}{5(k+2)}$, $D_k = \|w_k - y_k\|^2$, $p_k = \frac{100}{(k+1)^2}$.
7. For Algorithm 2 (in short iRSMEGM), we choose $\varpi_1 = 0.65$, $\theta = 0.60$, $\mu = 0.44$, $\kappa = 0.825$, $\tau = 0.825$, $\epsilon_k = \frac{1}{k^2}$, $\beta_k = \frac{1}{5(k+2)}$, $D_k = \|w_k - y_k\|^2$.

Example 4.1. To illustrate the effectiveness of our proposed Algorithm 1, we apply it to an image restoration problem. In this setting, each image consists of $D := M \times N$ pixels, with each pixel's intensity value ranging between $[0, 255]$, representing standard grayscale levels. We therefore model this setup in the real Hilbert space \mathbb{R}^D , where D corresponds to the total number of pixels, and endow this space with the Euclidean norm $\|\cdot\|$. We define the feasible set for pixel values as $\mathcal{C} = [0, 255]^D$, ensuring that all reconstructed values remain within realistic intensity bounds. Let \bar{x} denote the original (or true) image, and y^* represent the observed degraded image. The degradation process is modeled as follows:

$$y^* = A\bar{x} + \xi,$$

where A is a matrix representing the blurring effect, commonly referred to as the point spread function (PSF) or convolution matrix. The term ξ denotes an additive noise component, capturing random disturbances or imperfections in the observed image. The goal of image restoration is to reconstruct or closely approximate the original image \bar{x} , given the degraded observation y^* and the known blurring matrix A . This restoration task is formulated as a constrained optimization problem, aimed at minimizing the squared error between the degraded image and its estimated (blurred) counterpart:

$$\min_{x \in \mathcal{C}} \frac{1}{2} \|Ax - y^*\|^2.$$

Here, x denotes our estimate of the original image, and the objective function, $\frac{1}{2}\|Ax - y^*\|^2$, measures the discrepancy between the observed degraded image y^* and the estimated blurred image Ax . For clarity, we define this objective function as $\varphi(x)$, where:

$$\varphi(x) := \frac{1}{2}\|Ax - y^*\|^2.$$

Since A is a linear operator and the squared Euclidean norm $\|\cdot\|^2$ is convex, it follows that φ is also convex. This convexity allows us to reinterpret the constrained minimization problem as an equilibrium problem. Specifically, we define a bifunction B associated with this problem as follows:

$$B(x, y) := \varphi(y) - \varphi(x), \quad \forall x, y \in C.$$

This reformulation enables the application of equilibrium-based techniques to identify a solution that minimizes $\varphi(x)$ over the feasible set C . To evaluate the quality of the restored image x , we utilize the signal-to-noise ratio (SNR), a widely used metric in image processing. The SNR is expressed in decibels (dB) and is computed as follows:

$$\text{SNR} := 20 \log_{10} \frac{\|\bar{x}\|}{\|\bar{x} - x\|},$$

where \bar{x} represents the original image, and x is the restored image obtained by our method. A higher SNR value indicates that the restored image is closer to the original, thus reflecting a higher quality of restoration. For the initialization of our method, we select the initial point $x_0 = \mathbf{1} \in \mathbb{R}^D$ (a vector with all elements equal to 1) and set $x_1 = \mathbf{0} \in \mathbb{R}^D$ (a vector with all elements equal to 0).

We report the SNR as a function of both the iteration count and the CPU time required for each method, providing a dual perspective on the computational efficiency and effectiveness of each approach. By evaluating performance across these metrics, we aim to identify the strengths and weaknesses of the proposed method in comparison to existing techniques, offering insights into its applicability for real-world image recovery scenarios.

The aim of our numerical experiments is to evaluate the performance of the proposed Algorithm 1 in comparison with three established approaches (iPEGM, iSEGM, and iEGM). To ensure a comprehensive assessment, we simulate three distinct types of blurring and noise: *Motion Blur and Noise*, *Gaussian Blur and Noise*, and *Average Blur and Noise*. Each of these blurring techniques introduces specific distortions commonly encountered in real-world scenarios, enabling us to assess the robustness and efficiency of our method under various conditions. After applying the blurring, we implement our proposed approach as well as the existing methods to recover the degraded image, and compare the results based on restoration quality and computational efficiency.

Each of the chosen blurring techniques has unique characteristics and practical significance in image processing applications:

1. *Average Blur and Noise*: Average (or mean) blur reduces image details by averaging the values of neighboring pixels, resulting in a smoothing effect that diminishes noise but can also obscure fine details. This blurring technique is particularly relevant in applications where images undergo preprocessing steps such as downsampling or compression, which are common in fields like remote sensing and real-time video processing. The introduction of noise offers a more realistic test case, as average blur is frequently used to mitigate noise, often at the cost of unintentionally blurring important features. The numerical results corresponding to this technique are presented in Figs. 1 and 2.

2. *Motion Blur and Noise*: Motion blur simulates the effect of camera or object movement during image capture, typically resulting in elongated streaks in a specific direction. This type of blur is commonly encountered in dynamic imaging scenarios such as video recording, traffic surveillance, and sports photography. By adding noise, we replicate real-world conditions where motion blur is often accompanied by background noise, creating a challenging test case for image recovery methods. The numerical results corresponding to this technique are shown in Figs. 3 and 4.

3. *Gaussian Blur and Noise*: Gaussian blur, which applies a Gaussian function to smooth the image, is commonly employed in image processing to reduce detail and noise. In practical scenarios, this blurring effect may result from optical defocusing or low-quality imaging devices. Gaussian blur with added noise is frequently used in testing due to its widespread occurrence in applications such as medical imaging, satellite photography, and computer vision, where maintaining clarity and detail is crucial. The numerical results corresponding to this technique are presented in Figs. 5 and 6.

Example 4.2. This example is inspired by the Nash-Cournot oligopolistic equilibrium model, which describes the competition between firms in a market setting. The model and its mathematical structure are detailed in [8]. We now define a bifunction B that represents the interaction between two points x and y in the Hilbert space H as follows:

$$B(x, y) = \langle Px + Qy + c, y - x \rangle,$$

where $c \in \mathbb{R}^m$ is a constant vector, and P and Q are $m \times m$ matrices. The properties of the matrices are such that $Q - P$ is symmetric and negative semidefinite, and P is symmetric and positive semidefinite. Additionally, both matrices have a Lipschitz continuity constant given by $c_1 = c_2 = \frac{1}{2}\|P - Q\|$, as established in [8]. For practical computation in this numerical example, we use the following values for Q , P , and q :

$$Q = \begin{bmatrix} 1.6 & 1 & 0 & 0 & 0 \\ 1 & 1.6 & 0 & 0 & 0 \\ 0 & 0 & 1.5 & 1 & 0 \\ 0 & 0 & 1 & 1.5 & 0 \\ 0 & 0 & 0 & 0 & 2 \end{bmatrix}, \quad P = \begin{bmatrix} 3.1 & 2 & 0 & 0 & 0 \\ 2 & 3.6 & 0 & 0 & 0 \\ 0 & 0 & 3.5 & 2 & 0 \\ 0 & 0 & 2 & 3.3 & 0 \\ 0 & 0 & 0 & 0 & 3 \end{bmatrix},$$

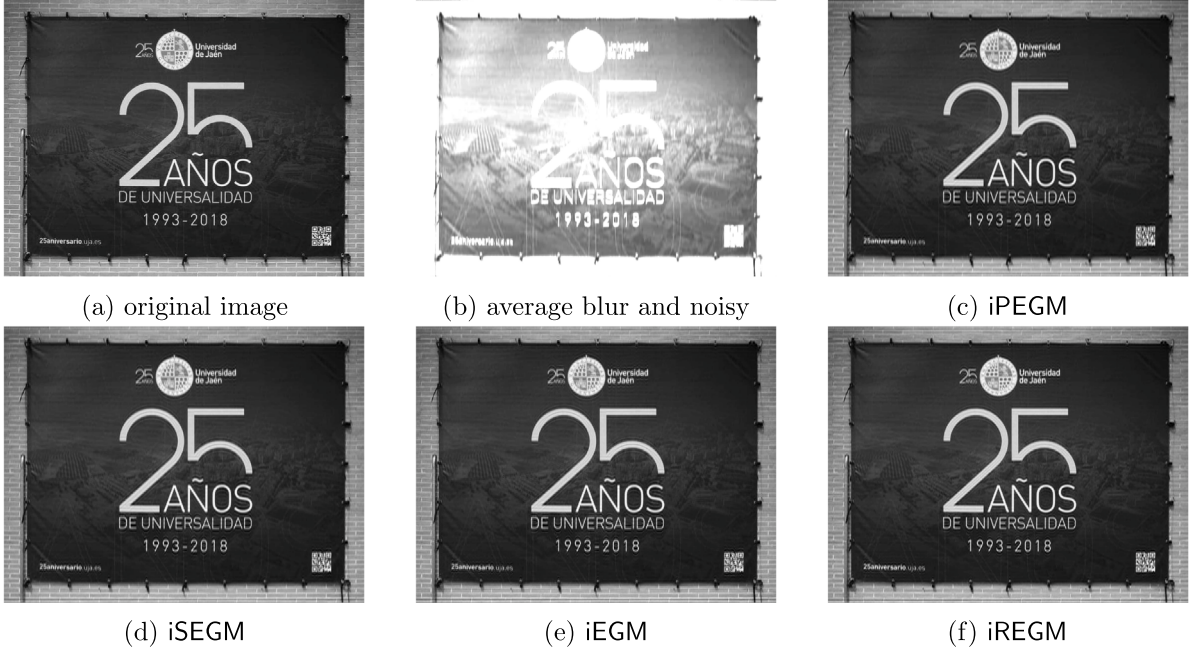


Fig. 1. Figure (a) displays the original image. Figure (b) depicts the image degraded by average blur and noise. Figure (c) shows the restored image generated by Algorithm 3.1 from [17], while Figure (d) illustrates the restored image obtained using Algorithm 2 from [19]. Figure (e) presents the restored image produced by Algorithm 1 from [18], and Figure (f) showcases the restored image generated by the proposed Algorithm 1.

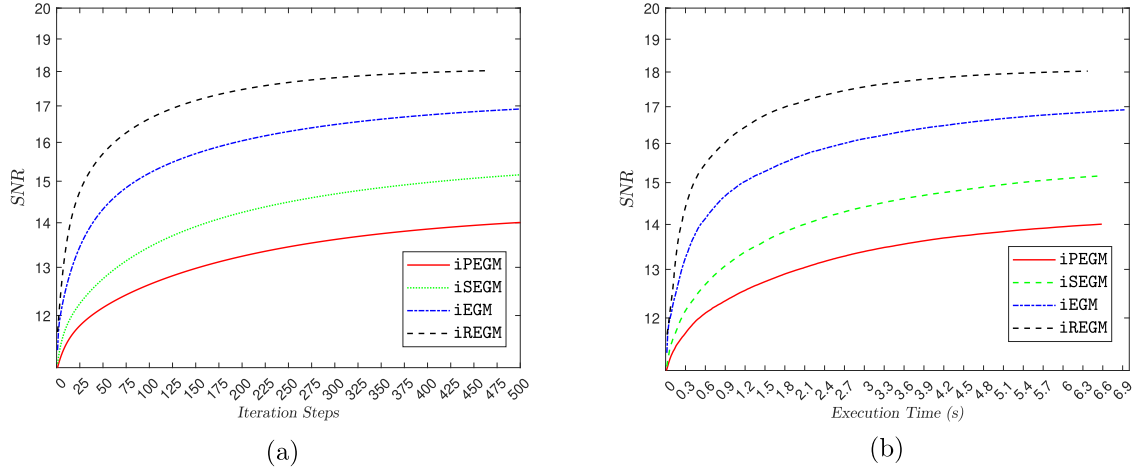


Fig. 2. Graphs (a) and (b) illustrate the relationship between SNR values and iteration count, and SNR values and CPU time, respectively, for the methods analyzed in Fig. 1.

$$q = [1, -2, -1, 2, -1]^T, \quad \text{and} \quad c = \frac{\|P - Q\|}{2}.$$

These choices for Q , P , q , and c satisfy the theoretical conditions necessary, allowing the algorithm to proceed.

Numerical experiments based on [Example 4.2](#) are conducted to evaluate the efficiency of Algorithms 1 and 2, focusing on CPU time (denoted by t in seconds) and the iteration count (k) required for convergence.

Experiment 1. In this experiment, the parameter x_0 is varied to compare the numerical performance of several algorithms: Algorithm 3.1 in [17], 2 in [19], Algorithm 1 in [18], and our Algorithm 1. [Figs. 7 and 8](#) and [Table 1](#) present the numerical results obtained for six distinct initial values of x_0 .

From [Figs. 7 and 8](#) and [Table 1](#), we observe the following:

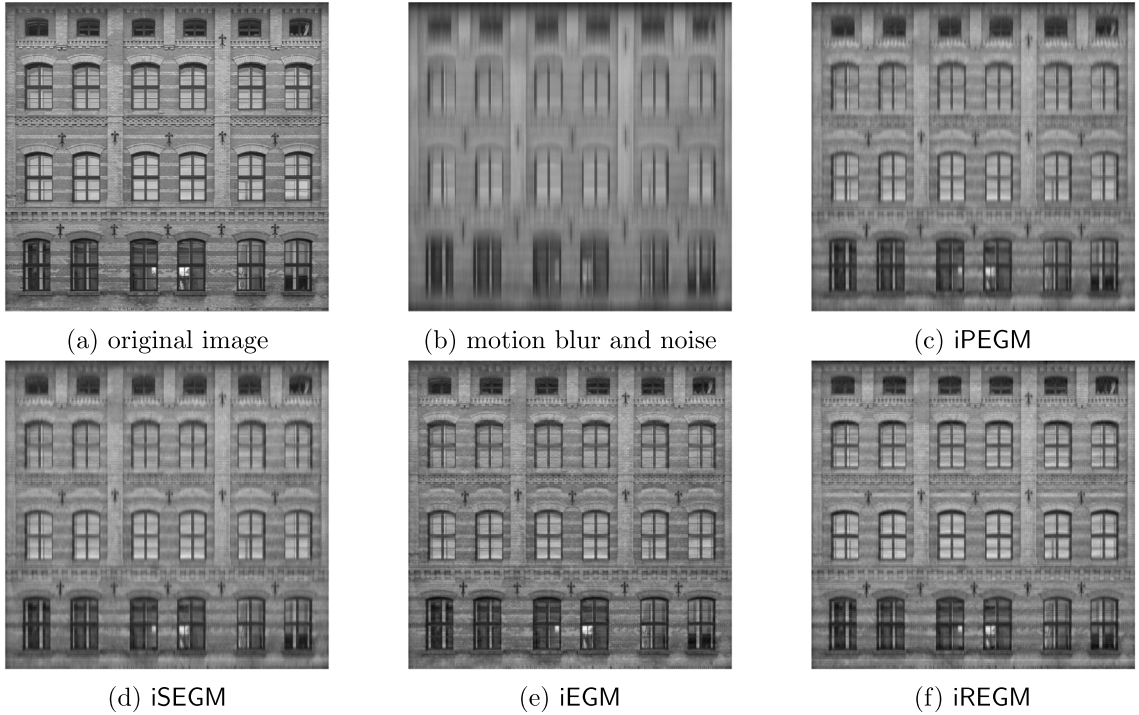


Fig. 3. Figure (a) displays the original image. Figure (b) depicts the image degraded by motion blur and noise. Figures (c)–(f) show the restored image generated by the methods described in Fig. 1.

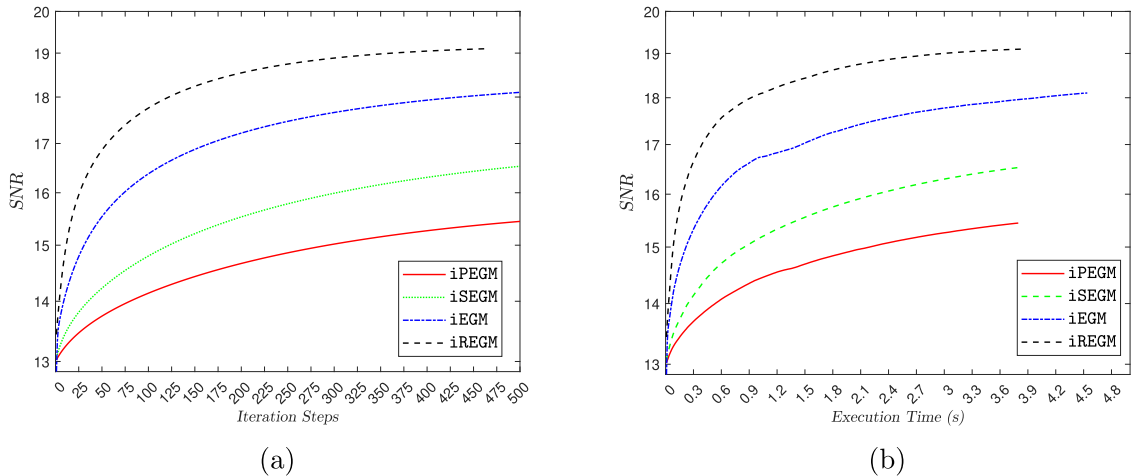


Fig. 4. Graphs (a) and (b) illustrate the relationship between SNR values and iteration count, and SNR values and CPU time, respectively, for the methods analyzed in Fig. 3.

- (i) For iREGM, as x_0 varies, the iteration count remains relatively low compared to the other algorithms. The counts for iREGM range between 22 and 28, indicating its efficiency in reaching convergence. In contrast, iPEGM, iSEGM, and iEGM generally require more iterations. Specifically, iPEGM and iSEGM reach up to 58 iterations for more variable initializations, such as $x_0 = [1, 2, 3, -4, 5]^\top$ and $x_0 = [2, -1, 3, -4, 5]^\top$, suggesting they are more sensitive to initial values.
- (ii) iREGM also performs well in terms of CPU time, consistently achieving the lowest times across most x_0 values, with a range from 0.310 to 0.381 s. This indicates that iREGM is computationally efficient, likely due to its lower iteration requirements. The other methods, especially iPEGM and iSEGM, show higher CPU times, particularly as x_0 becomes more varied.
- (iii) For iREGM, the initialization $x_0 = [0, 0, 0, 0, 0]^\top$ yields one of the lowest CPU times (0.310592 s) and an iteration count of only 22. This suggests that a simpler, neutral starting point minimizes computation time while maintaining a low iteration count.

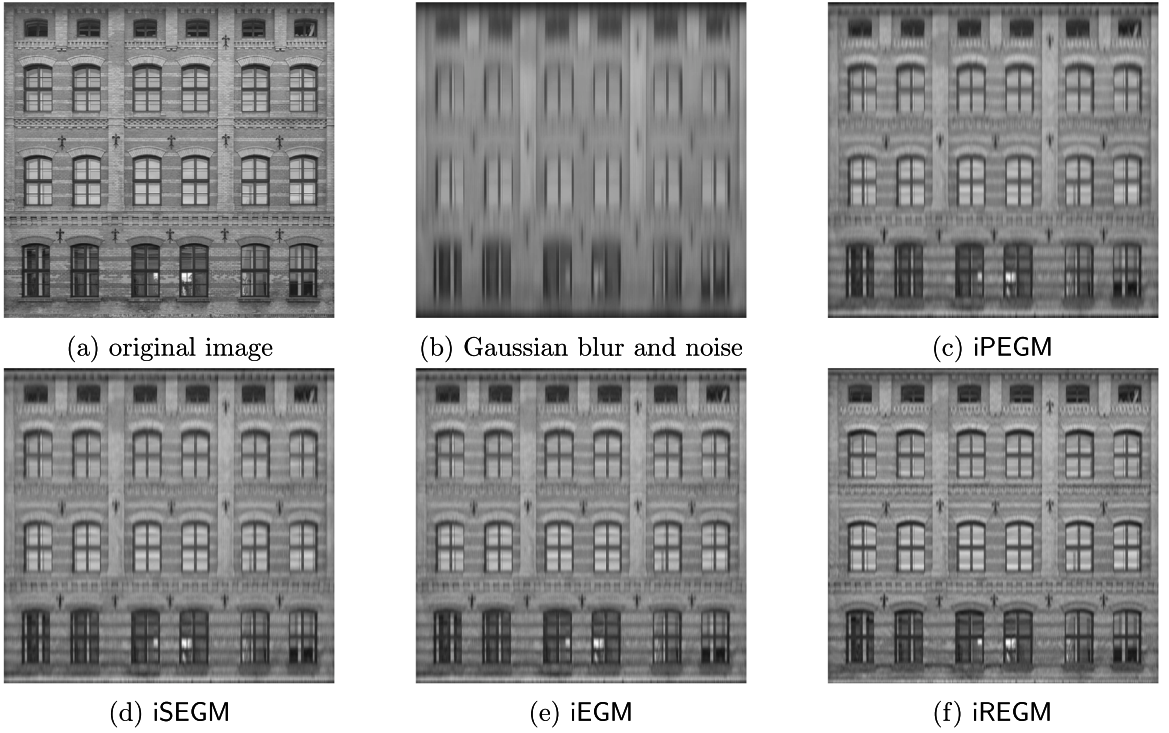


Fig. 5. Figure (a) displays the original image. Figure (b) depicts the image degraded by Gaussian blur and noise. Figures (c)–(f) show the restored image generated by the methods described in Fig. 1.

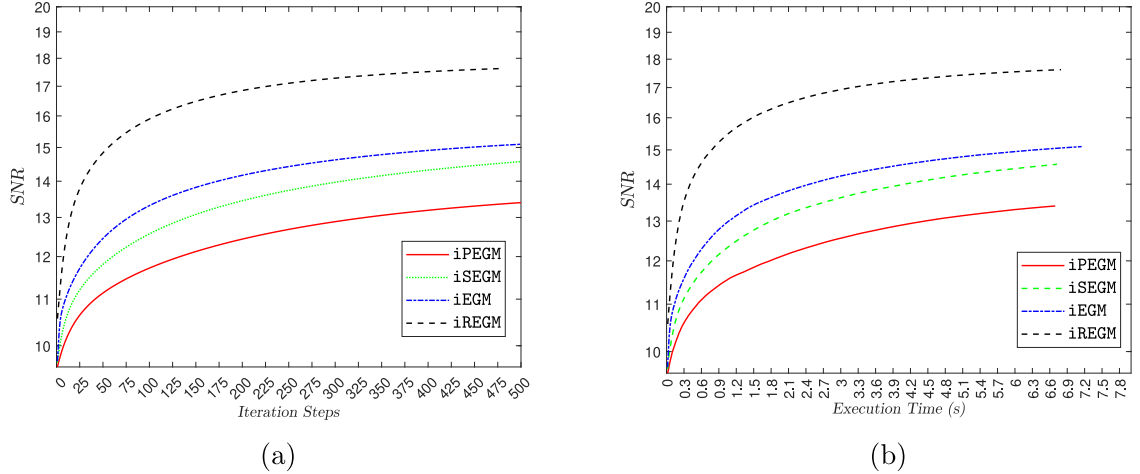


Fig. 6. Graphs (a) and (b) illustrate the relationship between SNR values and iteration count, and SNR values and CPU time, respectively, for the methods analyzed in Fig. 5.

Although slightly higher for other initializations, the iteration count and CPU time remain efficient, showing that iREGM is robust across different starting values.

- (iv) Overall, iREGM achieves a favorable balance between iteration count and CPU time across all tested values of x_0 . It consistently outperforms iPEGM, iSEGM, and iEGM in both metrics, highlighting its efficiency and reliability.

Experiment 2. This experiment evaluates the numerical performance of three algorithms: Algorithm 3 from [18], Algorithm 3.1 from [24], and our Algorithm 2 by varying the initial parameter x_0 . Figs. 9 and 10, along with Table 2, summarize the numerical results obtained for six distinct initial values of x_0 .

Based on these results, the following observations are made:

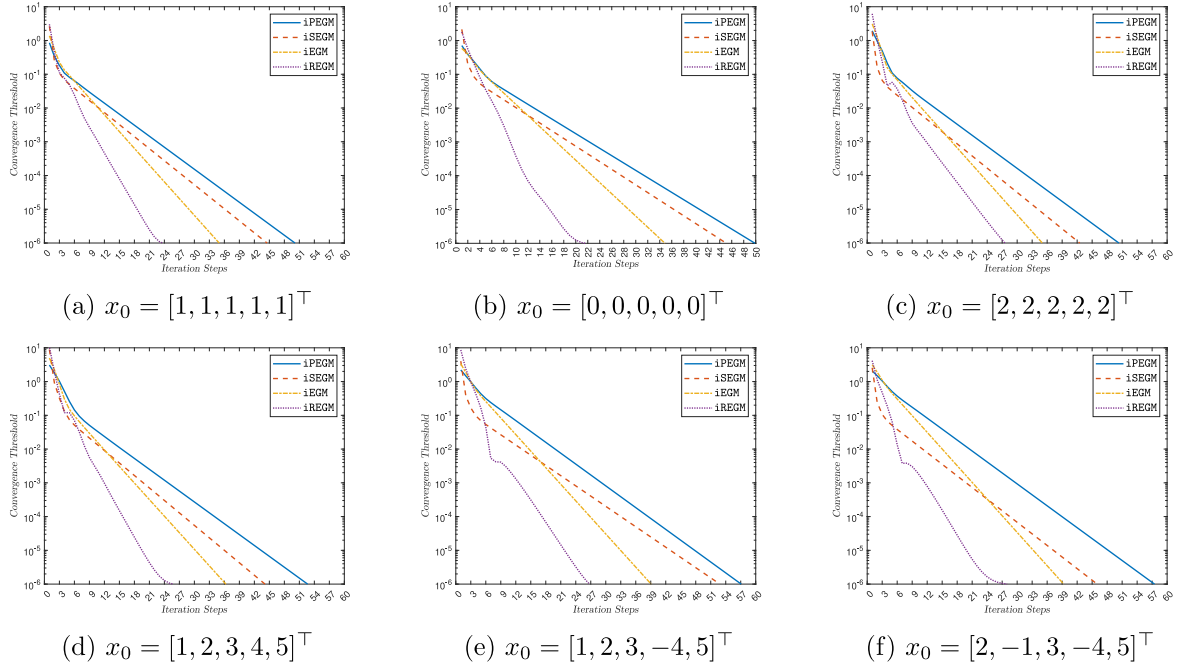


Fig. 7. Comparison of error term and iteration count for Algorithm 1 with other algorithms using various x_0 values in Experiment 1 of Example 4.2.

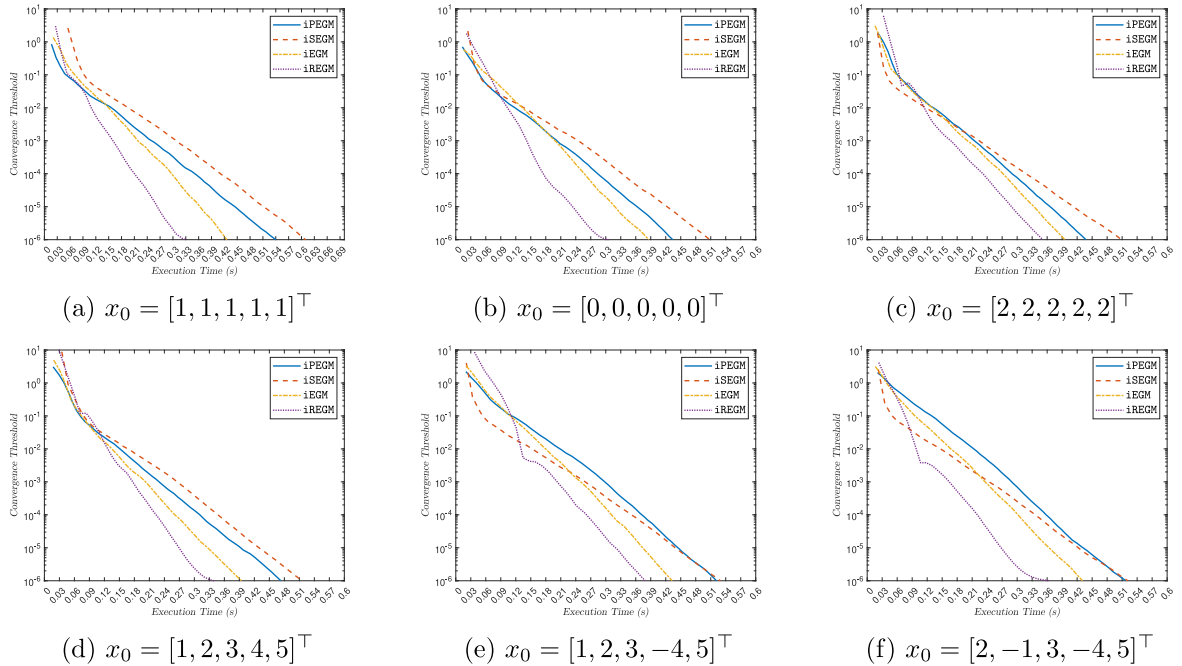


Fig. 8. Comparison of error term and elapsed time for Algorithm 1 with other algorithms using various x_0 values in Experiment 1 of Example 4.2.

- (i) For each initial point, iRSMEGM consistently exhibits the lowest iteration counts (k) compared to iMEGM and iSMEGM. For instance, with the initial point $[1, 1, 1, 1, 1]^\top$, iRSMEGM converges in 488 iterations, whereas iMEGM and iSMEGM require 707 and 592 iterations, respectively. This pattern suggests that iRSMEGM has more efficient convergence characteristics.

Table 1
Numerical data associated with Figs. 7 and 8.

x_0	iPEGM		iSEGM		iEGM		iREGM	
	k	t	k	t	k	t	k	t
$[1, 1, 1, 1, 1]^\top$	51	0.552324	45	0.614985	35	0.426293	24	0.334564
$[0, 0, 0, 0, 0]^\top$	50	0.435106	46	0.516347	35	0.387253	22	0.310592
$[2, 2, 2, 2, 2]^\top$	51	0.442636	43	0.515811	36	0.404221	28	0.321133
$[1, 2, 3, 4, 5]^\top$	53	0.475501	45	0.525171	37	0.401853	26	0.342597
$[1, 2, 3, -4, 5]^\top$	58	0.529097	53	0.530917	40	0.442222	27	0.381919
$[2, -1, 3, -4, 5]^\top$	58	0.522312	47	0.535435	40	0.437482	28	0.365248

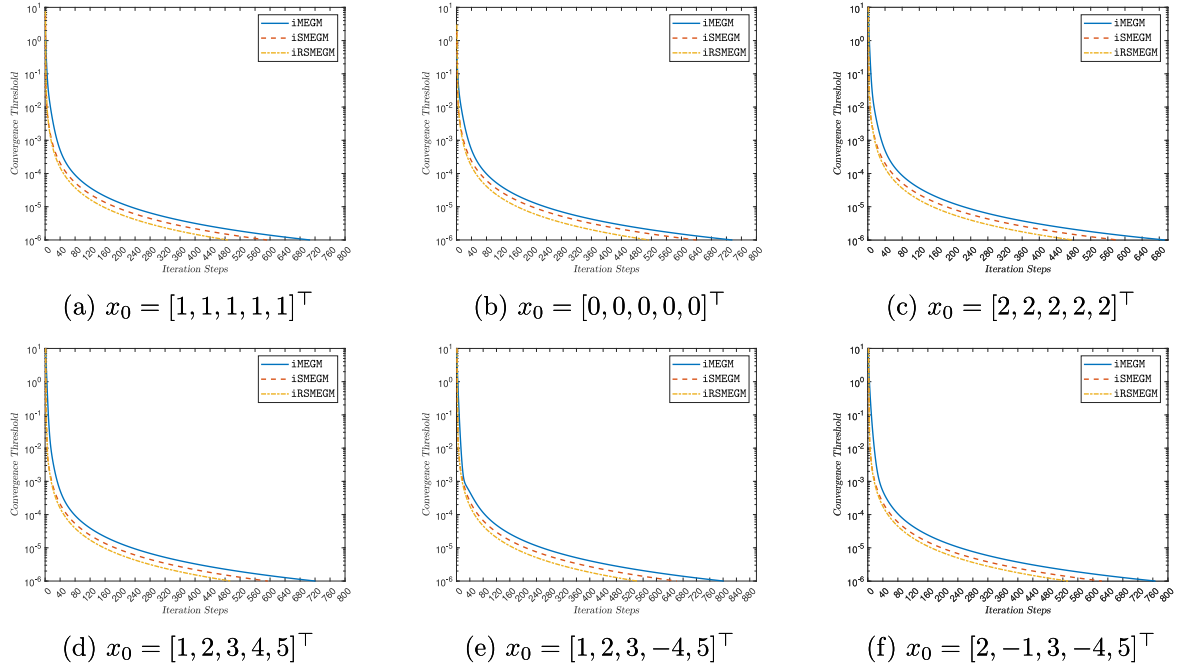


Fig. 9. Error term and iteration count for Algorithm 2, compared with other algorithms for various x_0 values in Experiment 2 of Example 4.2.

Table 2
Numerical data associated with Figs. 9 and 10.

x_0	iMEGM		iSMEGM		iRSMEGM	
	k	t	k	t	k	t
$[1, 1, 1, 1, 1]^\top$	707	7.592327	592	6.351945	488	5.301434
$[0, 0, 0, 0, 0]^\top$	736	7.316485	640	7.577108	513	6.288430
$[2, 2, 2, 2, 2]^\top$	693	6.808429	583	6.909141	478	5.165282
$[1, 2, 3, 4, 5]^\top$	721	7.190297	594	6.809648	496	6.009568
$[1, 2, 3, -4, 5]^\top$	802	7.998531	662	8.762895	542	6.779339
$[2, -1, 3, -4, 5]^\top$	767	7.376159	624	0.535435	534	7.344370

- (ii) In addition to fewer iterations, iRSMEGM generally requires less CPU time than the other methods. For example, with initial points $[1, 1, 1, 1, 1]^\top$ and $[2, 2, 2, 2, 2]^\top$, iRSMEGM achieves CPU times of 5.301434 and 5.165282 s, respectively, both of which are lower than the times recorded for iMEGM and iSMEGM.
- (iii) The choice of initial point influences both the iteration counts and CPU time across all algorithms. For instance, the initial point $[1, 2, 3, -4, 5]^\top$ increases both the iteration counts and CPU time for each method, with iRSMEGM requiring 542 iterations and 6.779339 s. This finding suggests that convergence speed is sensitive to the selection of the initial point.
- (iv) In summary, the results in Figs. 9 and 10, along with Table 2 demonstrate that iRSMEGM consistently outperforms the other two algorithms across different initial points, achieving fewer iterations and reduced CPU time in most cases.

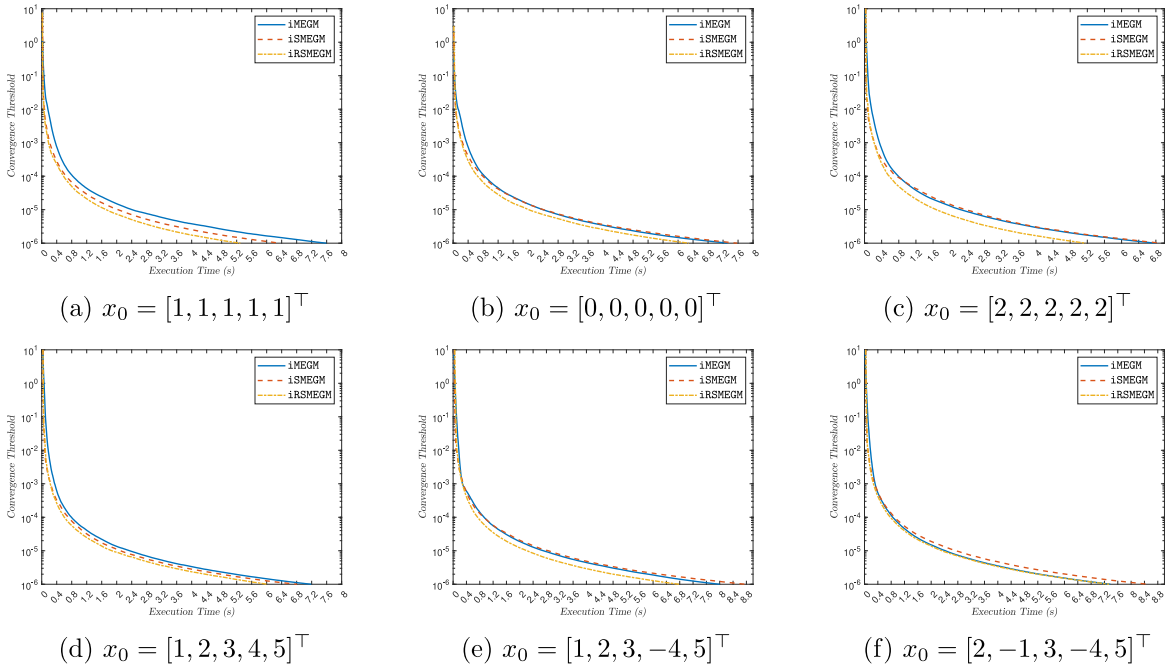


Fig. 10. Error term and elapsed time for Algorithm 2, compared with other algorithms for various x_0 values in Experiment 2 of Example 4.2.

5. Conclusions

In this paper, we introduce two inertial algorithms to solve equilibrium problems in real Hilbert spaces. Under suitable conditions, the weak convergence and strong convergence theorems of the proposed algorithms are established, respectively. Finally, numerical experiments, including applications in image restoration problems, demonstrate the computational advantages of the proposed algorithms compared to other methods. In future work, we consider extending the proposed algorithms to solve equilibrium problems on Hadamard manifolds.

CRediT authorship contribution statement

Habib ur Rehman: Writing – review & editing, Writing – original draft, Validation, Software, Methodology, Investigation, Formal analysis, Conceptualization. **Bing Tan:** Writing – review & editing, Writing – original draft, Investigation, Funding acquisition, Formal analysis, Conceptualization. **Jen-Chih Yao:** Writing – review & editing, Writing – original draft, Supervision, Formal analysis, Conceptualization.

Declaration of competing interest

The authors declare the following financial interests/personal relationships which may be considered as potential competing interests: Bing Tan reports financial support was provided by Natural Science Foundation Project of Chongqing. Bing Tan reports financial support was provided by Fundamental Research Funds for the Central Universities. If there are other authors, they declare that they have no known competing financial interests or personal relationships that could have appeared to influence the work reported in this paper.

Acknowledgments

The authors are very grateful to the Handling Editor and four reviewers for their suggestions, which helped us improve the readability and clarity of the paper. Bing Tan thanks the support of the Fundamental Research Funds for the Central Universities (No. SWU-KQ24052, No. SWU-KR25013), the Natural Science Foundation of Chongqing (No. CSTB2024NSCQ-MSX0354), and the Natural Science Foundation of China (No. 12471473).

Data availability

No data was used for the research described in the article.

References

- [1] Konnov IV. Equilibrium models and variational inequalities. Vol. 210, Elsevier; 2007.
- [2] Han W. An introduction to theory and applications of stationary variational-hemivariational inequalities. Springer Nature; 2024.
- [3] Nash JF. Equilibrium points in n-person games. Proc Natl Acad Sci 1950;36:48–9.
- [4] Cohen G. Auxiliary problem principle and decomposition of optimization problems. J Optim Theory Appl 1980;32:277–305.
- [5] Cohen G. Auxiliary problem principle extended to variational inequalities. J Optim Theory Appl 1988;59:325–33.
- [6] Mastroeni G. On auxiliary principle for equilibrium problems. In: Nonconvex optimization and its applications. Springer US; 2003, p. 289–98.
- [7] Flåm SD, Antipin AS. Equilibrium programming using proximal-like algorithms. Math Program 1996;78:29–41.
- [8] Quoc-Tran D, Dung ML, Nguyen VH. Extragradient algorithms extended to equilibrium problems. Optim 2008;57:749–76.
- [9] Korpelevich GM. The extragradient method for finding saddle points and other problems. Matekon 1976;12:747–56.
- [10] Censor Y, Gibali A, Reich S. The subgradient extragradient method for solving variational inequalities in Hilbert space. J Optim Theory Appl 2011;148:318–35.
- [11] Censor Y, Gibali A, Reich S. Strong convergence of subgradient extragradient methods for the variational inequality problem in Hilbert space. Optim Methods Softw 2011;26:827–45.
- [12] Censor Y, Gibali A, Reich S. Extensions of korpelevich's extragradient method for the variational inequality problem in Euclidean space. Optim 2012;61:1119–32.
- [13] Polyak B. Some methods of speeding up the convergence of iteration methods. USSR Comput Math Math Phys 1964;4:1–17.
- [14] Nesterov Y. A method for unconstrained convex minimization problem with the rate of convergence $O(1/k^2)$. Dokl Akad Nauk SSSR 1983;269:543–7.
- [15] Alvarez F, Attouch H. An inertial proximal method for maximal monotone operators via discretization of a nonlinear oscillator with damping. Set- Valued Anal 2001;9:3–11.
- [16] Hieu DV. An inertial-like proximal algorithm for equilibrium problems. Math Methods Oper Res 2018;88:399–415.
- [17] Hieu DV, Cho YJ, Xiao Y. Modified extragradient algorithms for solving equilibrium problems. Optim 2018;67:2003–29.
- [18] Vinh NT, Muu LD. Inertial extragradient algorithms for solving equilibrium problems. Acta Math Vietnam 2019;44:639–63.
- [19] Hu Rehman, Kumam P, Cho YJ, Yardsorn P. Weak convergence of explicit extragradient algorithms for solving equilibrium problems. J Inequal Appl 2019;2019:243.
- [20] Hu Rehman, Kumam P, Cho YJ, Suleiman YI, Kumam W. Modified popov's explicit iterative algorithms for solving pseudomonotone equilibrium problems. Optim Methods Softw 2021;36:82–113.
- [21] Hu Rehman, Ghosh D, Yao JC, Zhao X. Extragradient methods with dual inertial steps for solving equilibrium problems. Appl Anal 2024;103:2941–76.
- [22] Shehu Y, Dong QL, Liu L, Yao JC. Alternated inertial subgradient extragradient method for equilibrium problems. TOP 2023;1–30.
- [23] Wang K, Wang Y, Iyiola OS, Shehu Y. Double inertial projection method for variational inequalities with quasi-monotonicity. Optim 2024;73:707–39.
- [24] Hu Rehman, Kumam P, Shehu Y, Ozdemir M, Kumam W. An inertial non-monotonic self-adaptive iterative algorithm for solving equilibrium problems. J Nonlinear Var Anal 2022;6:51–67.
- [25] Lyashko SI, Semenov VV, Voitova TA. Low-cost modification of korpelevich's methods for monotone equilibrium problems. Cybernet Systems Anal 2021;47:631–9.
- [26] Yang J, Liu H. The subgradient extragradient method extended to pseudomonotone equilibrium problems and fixed point problems in Hilbert space. Optim Lett 2020;14:1803–16.
- [27] Shehu Y, Iyiola OS, Thong DV, Van NTC. An inertial subgradient extragradient algorithm extended to pseudomonotone equilibrium problems. Math Methods Oper Res 2021;93:213–42.
- [28] Jolaoso LO. The subgradient extragradient method for solving pseudomonotone equilibrium and fixed point problems in Banach spaces. Optimization 2022;71:4051–81.
- [29] Yao Y, Adamu A, Shehu Y, Yao JC. Simple proximal-type algorithms for equilibrium problems. J Global Optim 2024;89:1069–98.
- [30] Thong DV, Cholamjiak P, Rassias MT, Cho YJ. Strong convergence of inertial subgradient extragradient algorithm for solving pseudomonotone equilibrium problems. Optim Lett 2022;16:545–73.
- [31] Cholamjiak W, Dutta H, Yambangwai D. Image restorations using an inertial parallel hybrid algorithm with Armijo linesearch for nonmonotone equilibrium problems. Chaos Solitons Fractals 2021;153:111462.
- [32] Babu F, Ali A, Alkhaldi AH. An extragradient method for non-monotone equilibrium problems on Hadamard manifolds with applications. Appl Numer Math 2022;180:85–103.
- [33] Shehu Y, Liu L, Qin X, Dong QL. Reflected iterative method for non-monotone equilibrium problems with applications to Nash-cournot equilibrium models. Netw Spat Econ 2022;22:153–80.
- [34] Thang TV, Le XT. Self-adaptive extragradient algorithms for quasi-equilibrium problems. J Optim Theory Appl 2024;203:2988–3013.
- [35] Bianchi M, Schaible S. Generalized monotone bifunctions and equilibrium problems. J Optim Theory Appl 1996;90:31–43.
- [36] Van Tiel J. Convex analysis: an introductory text. New York: Wiley; 1984.
- [37] Tan K, Xu H. Approximating fixed points of nonexpansive mappings by the ishikawa iteration process. J Math Anal Appl 1993;178:301–8.
- [38] Opial Z. Weak convergence of the sequence of successive approximations for nonexpansive mappings. Bull Amer Math Soc 1967;73:591–7.